(2)

GA-C19465
3/90

HIGH TEMPERATURE CERAMIC SUPERCONDUCTORS

FOR PERIOD
JANUARY 1, 1990 – MARCH 31, 1990

Prepared for
OFFICE OF NAVAL RESEARCH
800 North Quincy Street
Arlington, VA 22217-5000
DARPA/ONR Contract N00014-88-C-0714

Prepared by
K.S. MAZDIYASNI, PROGRAM MANAGER (619) 455-4587
A. CHEN
K.C. CHEN
D.M. DUGGAN
F.C. MONTGOMERY
S.S. PAK
M.B. MAPLE, UCSD
L. PAULIUS, UCSD
P. TSAI, UCSD

APPROVED BY: T.D. Gulden
T.D. GULDEN
DIRECTOR, DEFENSE MATERIALS

The views and conclusions contained in this quarterly report are those of the authors and should not be interpreted as necessarily representing the official policies, either expressed or implied, of the Defense Advanced Research Project Agency of the U.S. Government.

GENERAL ATOMICS PROJECT 3850
APRIL 10, 1990

GENERAL ATOMICS

CONTENTS

FIGURES

FIGURES (Continued)

FIGURES (Continued)

TABLES

1. INTRODUCTION

This is the fifth quarterly progress report on the work performed in the period from January 1, 1990 through March 31, 1990 on Office of Naval Research (ONR) Contract N00014-88-C-0714, entitled "High-Temperature Ceramic Superconductors." The principal objectives of this program are (1) to demonstrate fabrication of high-temperature ceramic superconductors that can operate at or above 90 K with appropriate current density, J_c, in forms useful for application in resonant cavities, magnets, motors, sensors, computers, and other devices; and (2) to fabricate and demonstrate selected components made of these materials, including microwave cavities and magnetic shields.

1.1. PROJECT OUTLINE

This program consists of six tasks: (1) metal alkoxide synthesis and processing, (2) microstructural evaluation and property measurement, (3) electrical and magnetic property measurement, (4) superconductor ceramic processing, (5) component fabrication and demonstration, and (6) reporting.

Task 1 is to synthesize a homogeneous alkoxide solution that contains all the constituent elements that can be easily made into powders, thin film, or drawn into fiber form. Ideally, this solution should possess precise stoichiometry, adequate stability, polymerizability, adherence, and spinnability. Also, the polymeric materials formed from this solution should be thermosetting, be able to be dissolved in organic solvents, and contain as little as possible low-temperature pyrolyzable organics with high char yield.

Task 2 is to study the microstructure as a function of processing parameters. The study includes: density, pore size, and pore size distribution, phase identification, chemical composition and purity, environmental stability, effects of heat treatment, residual strain, seeding, annealing in magnetic fields, and epitaxy on grain growth and orientation.

Task 3 is to study the electrical and magnetic properties of the $YBa_2Cu_3O_7$ (123) high T_c ceramic superconductors. it will include both the ac electrical resistance (R_{ax}) and the ac magnetic susceptibility (χac).

Task 4 is to investigate superconductor ceramic processing. Most of the important applications of superconductors require material in the form of fiber or films. Magnets, conductors, motors, and generators are examples of applications employing fiber; while detectors, microwave cavities, and microcircuitry require superconducting material in the form of films. The sol-gel process is ideally suited to producing materials in these forms; in fact, it is used commercially to produce ant-reflection and mirror coatings and to produce continuous ceramic fibers for structural reinforcement in composite materials and for thermal insulation.

Task 5 is to demonstrate component fabrication. General Atomics (GA) will design and build a high Q, high Tc superconducting cavity, using its unique sol-gel coating process capabilities. This task will proceed after some initial coating tests have verified dc superconductivity and after we have answered questions of adhesiveness, surface preparation, and processing procedures. As the fabrication process and the materials quality are improved throughout the three-year program, two additional cavities will be constructed and tested. Coupling will be through a waveguide inductive iris into an end wall, with a logarithmic decrement technique of Q measurement considered most appropriate

for the high Q anticipated. An X-band (10 GHz) frequency choice allows for convenient dimensions of 4.3 cm diameter by 2.8 cm height.

This report will focus primarily on Tasks 2, 3, 4, and 5.

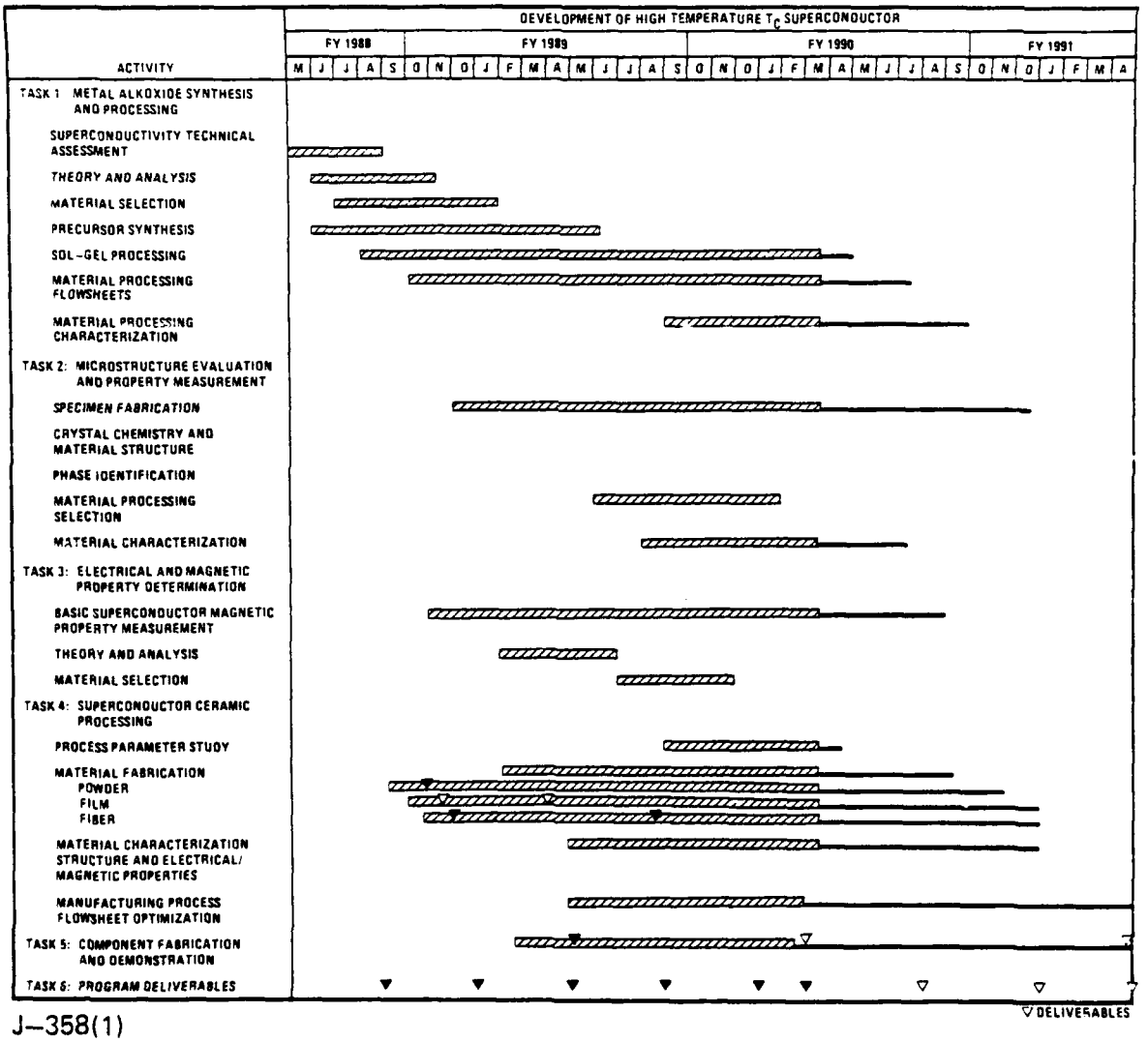

J–358(1)
4–18–90

2. THIN FILM AND FIBER PROCESSING

During this reporting period, homogeneous solutions have been prepared using $Y(OR)_3$, $Ba(OR)_2$, and the copper (II) mixed-ligand species $(C_5H_7O_2)_2Cu_2(u\text{-}OR)_2$, where R = $CH_2CH_2OCH_2CH_2OCH_2CH_3$ and $C_5H_7O_2$ = 2, 4 - pentanedionate.

2.1. EXPERIMENTAL PROCEDURE

The starting alkoxides, and the mixed-ligand copper (II) compound were prepared using the procedure described in the previous progress report.

2.1.1. Preparation of 123 Precursor Solution

A septum bottle containing the required stoichiometric solution of yttrium, barium and copper was prepared by weighing aliquots of the stock alkoxide solutions. The alkoxides were hydrolyzed using less than 2 moles of water per mole of metal by injecting a dilute solution of the required amount of water in 2-(2-ethoxyethoxy)ethanol into the alkoxide solution. The sample was heated in an oil bath at 55°C for four hours, then concentrated at the same temperature under reduced pressure. The final weight percent of equivalent 123 in the homogeneous solution was adjusted by adding dry 2-(ethoxyethoxy) ethanol.

2.1.2. Dip Coating

Thin strips of yttria stabilized zirconia polycrystal (YSZP), nickel and silver have been coated with the precursor solution. Dip coating was conducted in a small bench-top coater under dry nitrogen to reduce the chance of $BaCO_3$ formation. The substrates were vertically dipped for 10 s, withdrawn from the solution at 0.38 mm/s, and fired at

400-600 °C for 3 minutes before repeating the cycle. For most precursor solutions, four dips were required to fill the void space caused during the drying process.

123 is known to react, at temperatures in excess of 900°C, with nickel metal[2]. To reduce the rate of this reaction, a barrier layer of Y_2O_3 was deposited by sol-gel method on some of the nickel strips. This layer was deposited by dip-coating from a partially hydrolyzed solution of yttrium tris-2-(ethoxy)ethoxide. An SEM photomicrograph of the coating is shown in Fig. 1. The crystallites are randomly oriented with an average size of approximately 1μm.

2.1.3. Electrical Property Measurements

D.C. susceptibility measurements were conducted at GA on samples about 3-5 mm wide and 5-10 mm long.

Resistance measurements were conducted at The University of California, San Diego (UCSD) using a Linear Research LR-400 Four Wire Ac Resistance Bridge, with a current of 0.1 uA at 13 Hz. Silver wire leads were cemented to the 123 film with silver paste after sputtering 1 mm x 3 mm silver pads on the coating. The pads were positioned by preparing an aluminum foil mask which surrounded the sample piece. The current pads were spaced 1 mm from the voltage pads, and the voltage pads were 4 mm apart. Thus, about 13 mm^2 of the film was tested.

2.1.4. Results and Discussion

Coherent films are formed on YSZP, nickel and silver. As deposited, these films appear glossy black, are amorphous, and show no structure in either an optical microscope at 1000x magnification, or in the SEM at a magnification of 4000x. The thermal anneal process, however, causes crystallization, and grain growth and the film becomes a

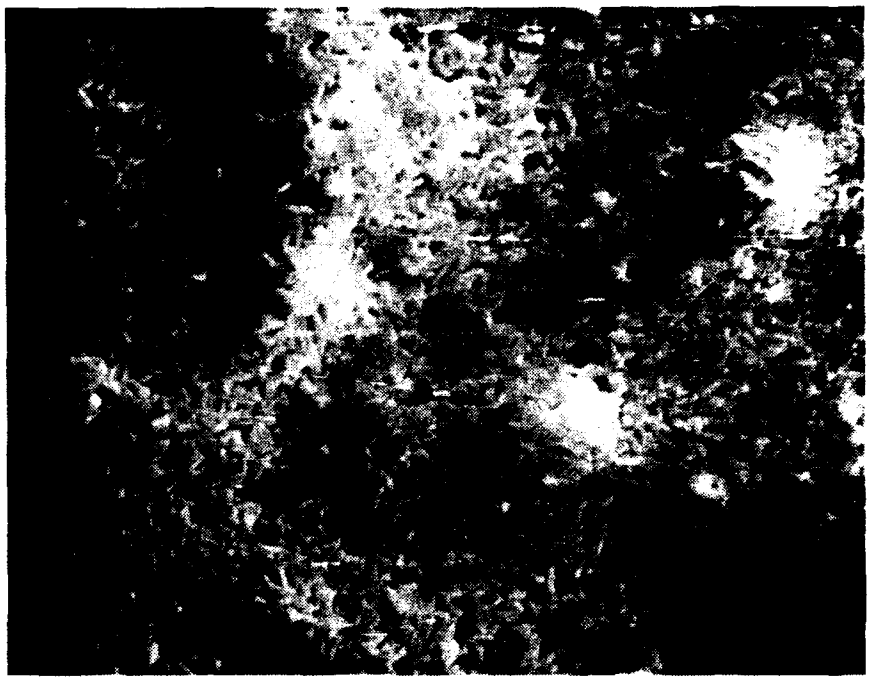

Fig. 1. SEM photograph of Y_2O_3 barrier layer on nickel foil

diffuse black. Figure 2 is a photograph of 123 films on yttria coated nickel showing these changes in the appearance of the films.

Characterization of film electrical properties has been difficult because of the small amount of superconductor deposited on the substrate. Furthermore, D.C. susceptibility measurements are hard to interpret because the response of the substrate material changes for different barrier layers and is, in most cases larger than the susceptibility of the film. An example of the susceptibility data obtained from coatings on YSZP is shown in Fig. 3. For the superconducting sample (30 Oe), the onset of superconductivity is between 80 and 90 K, with T_{50} = 74 K and T_{10} = 34 K. This film had been heated in ultrapure oxygen to 922°C at 1°C/min, held for 10 min, cooled to 435°C and held for 5 hours.

Samples which had been processed to 900°C or lower did not show a Meissner effect. The second film in Fig. 3 did not expel magnetic field from room temperature down to about 4 K. This film had been heated to 884°C in ultrapure oxygen at the same rate as the other sample. However, this sample was oxygenated at 485°C for only 1 hour. For bulk samples, the extent of oxygenation increases with extended anneals at temperatures around 400°C. Thus, it is possible that this sample could have been substoichiometric in oxygen.

The processing conditions also appear to affect the electrical resistance of the films. In the following discussion, it is assumed that the processing conditions altered the electrical properties of the films. However, it is possible that aging effects in the precursor solution may have changed the solution stoichiometry or chemistry. Additional tests are in progress to confirm the conclusions reported below.

In Fig. 4, the effect of 10 minute anneals at temperatures exceeding 900°C is shown. The figure plots the temperature dependence of the

Fig. 2. Sol-gel solution condensed thin film on sol-gel Y_2O_3 coated Ni substrate, a) before sintering, b) after sintering

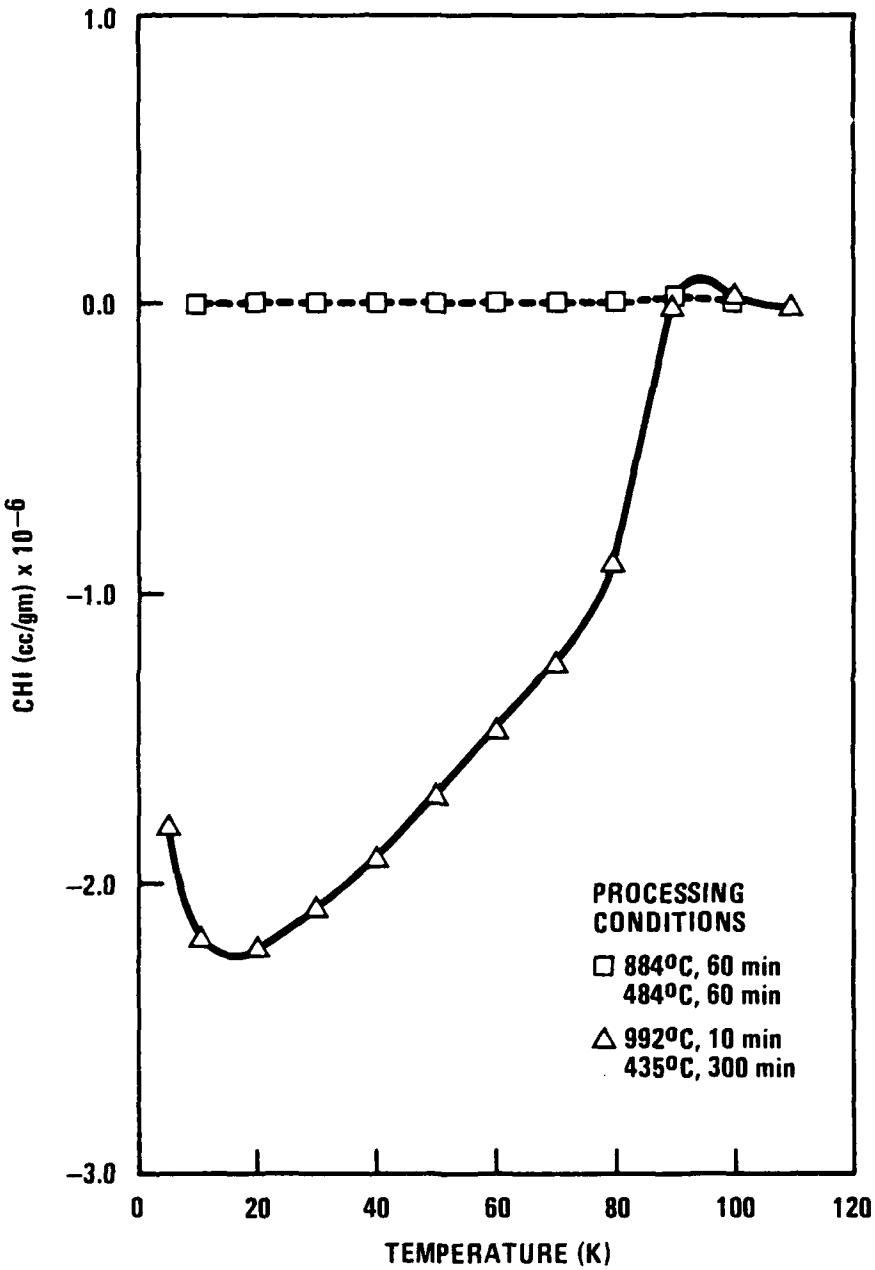

Fig. 3. D.C. susceptibility of films on yttria-coated nickel

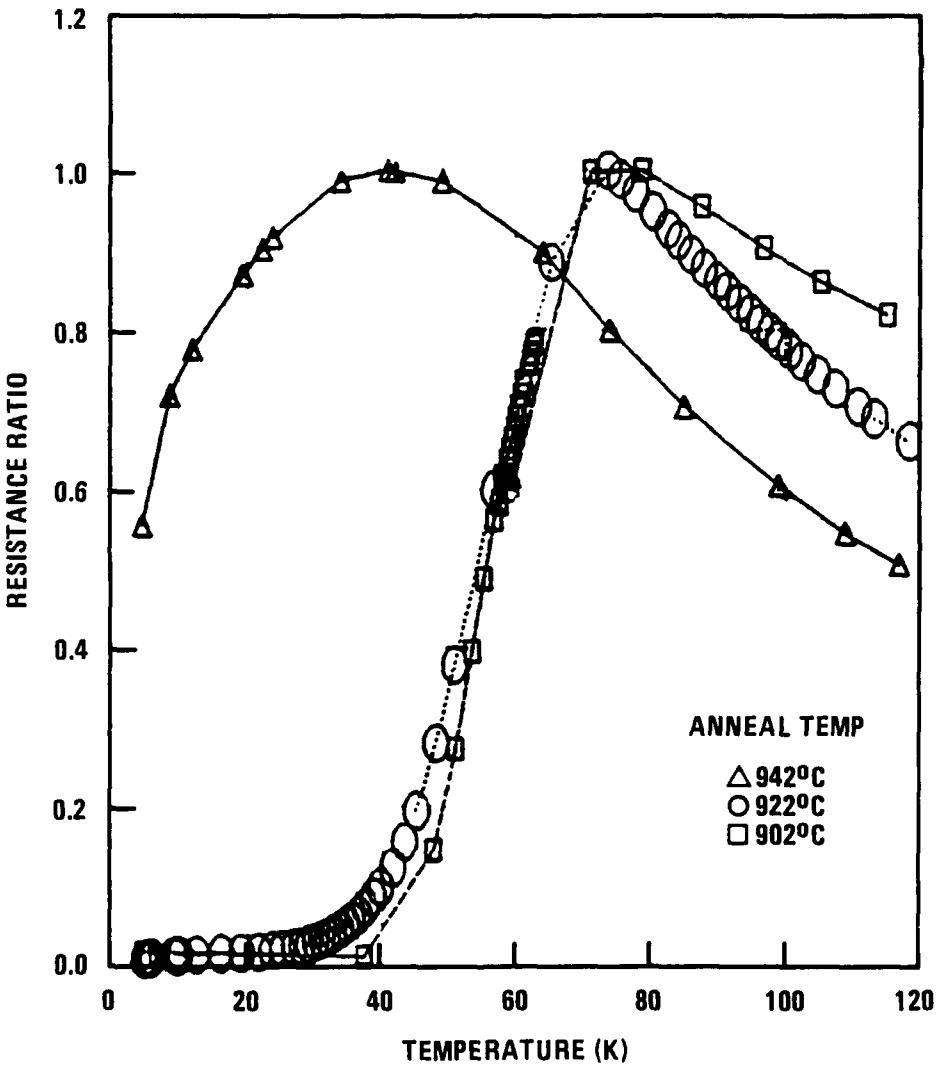

Fig. 4. Effect of processing temperature on the resistance of films on nickel.

ratio of the film. All of the samples tested exhibit a region of semiconducting behavior (an increase in the resistance as the temperature of the film is lowered). However, in several samples, a broad superconducting transition occurred below a critical temperature.

The amount of semiconducting behavior, the sharpness of the transition, and the critical temperature depend on the processing conditions. Films annealed for 10 minutes above 920°C show a significant increase in the room temperature resistance, and are more semiconducting than samples annealed around 900°C. Although the room temperature resistance is affected by film thickness, each of the test films were produced by four dips of the substrate. This suggests that perhaps an impurity reaction layer forms during processing at the interface of the film and the substrate. The fact that a film on clean nickel heated to only 903°C also was semiconducting down to 4 K supporting the interface reaction.

The type of barrier layer on the nickel substrate also influences the film resistance. Resistance data for four films which had been heated to 942°C, held for 10 minutes, cooled to 434°C and held for 5 hrs is given in Fig. 5. The film on clean nickel, and the film on yttria coated nickel that had <u>not</u> been annealed before deposition of the 123 layer, are semiconducting throughout the temperature region tested. The superconducting transition of a film on yttria coated nickel which had been annealed at 900°C prior to deposition of the 123 was around 40 K. Finally, the transition of a film on oxidized nickel began around 58 K. It is conjectured that a low melting liquid could have been formed which dissolved the base metal easier than the oxide coatings.

The SEM macrostructure and the microstructure of superconducting films and semiconducting films obtained with different processing parameters are shown in Figs. 6 through 9. The films formed on YSZP, shown in Figs. 6 and 7, have pock marks which appear to have been caused by bubbling. These defects in the film macrostructure do not seem to affect the onset of the superconducting transition, since the pocks are

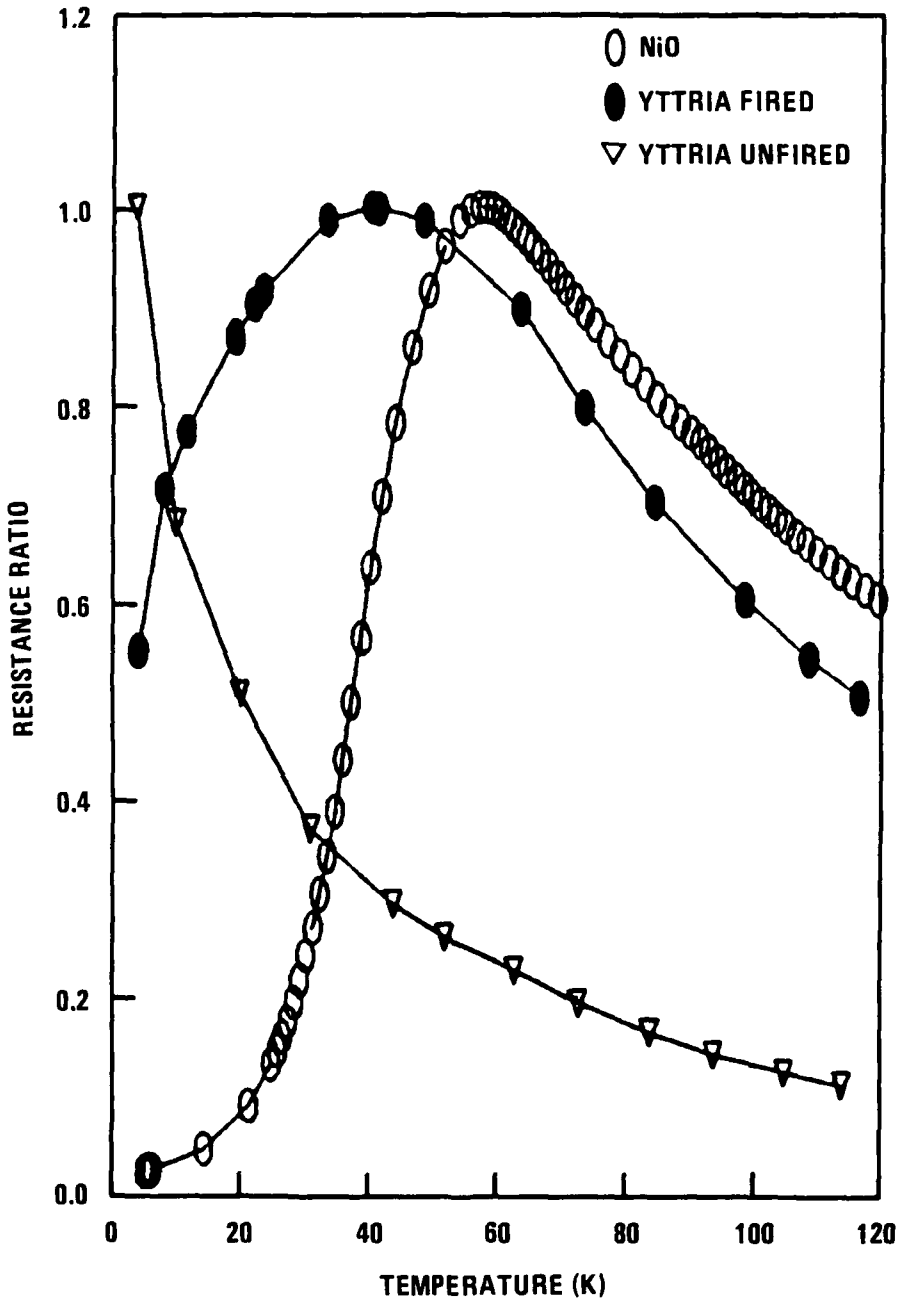

Fig. 5. Effect of barrier layer on resistance of films on nickel

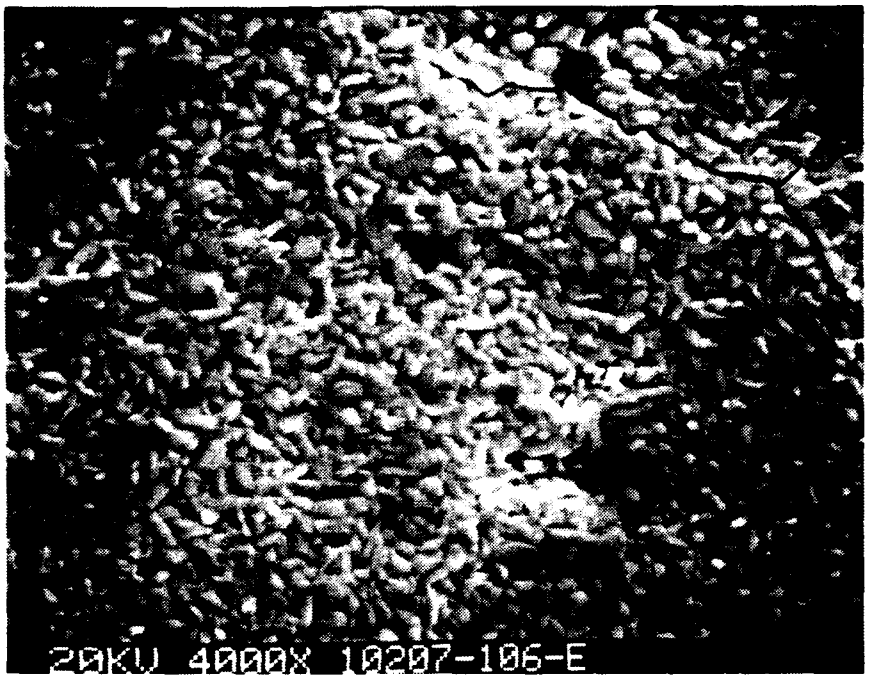

4000 x

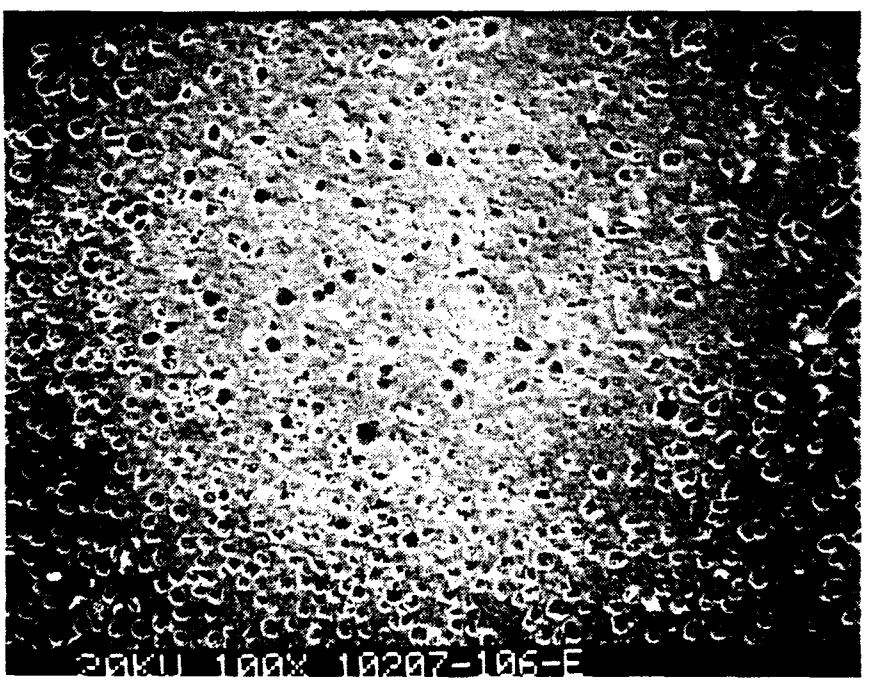

100 x

Fig. 6. SEM photographs showing microstructure of films on YSZP which did not exhibit Meissner effect

4000 x

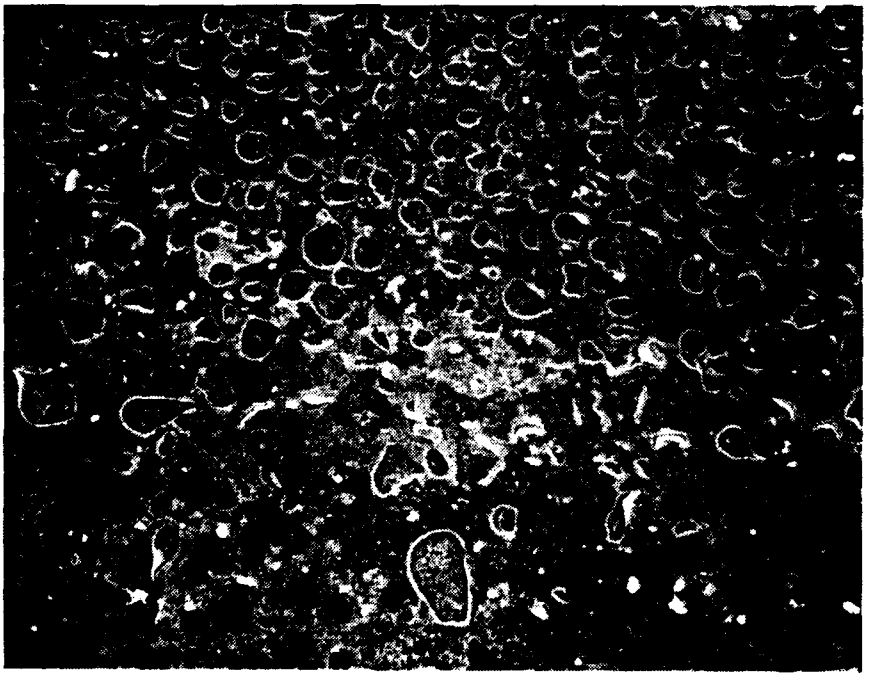

100 x

Fig. 7. SEM photographs showing microstructure of superconducting film on YSZP

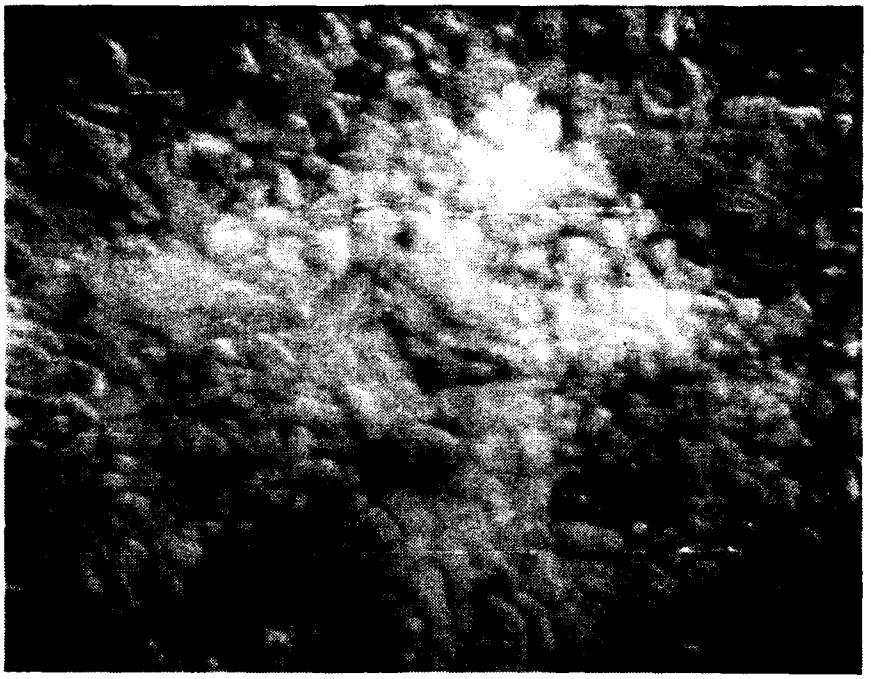

10,000 x

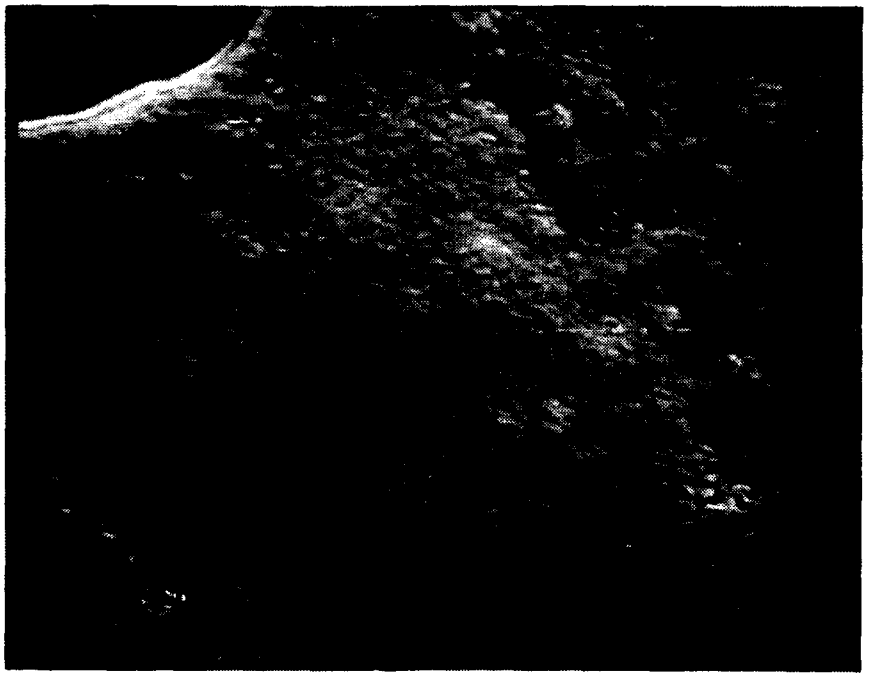

4000 x

Fig. 8. SEM photographs showing microstructure of superconducting film on yttria-coated nickel heated to 903°C

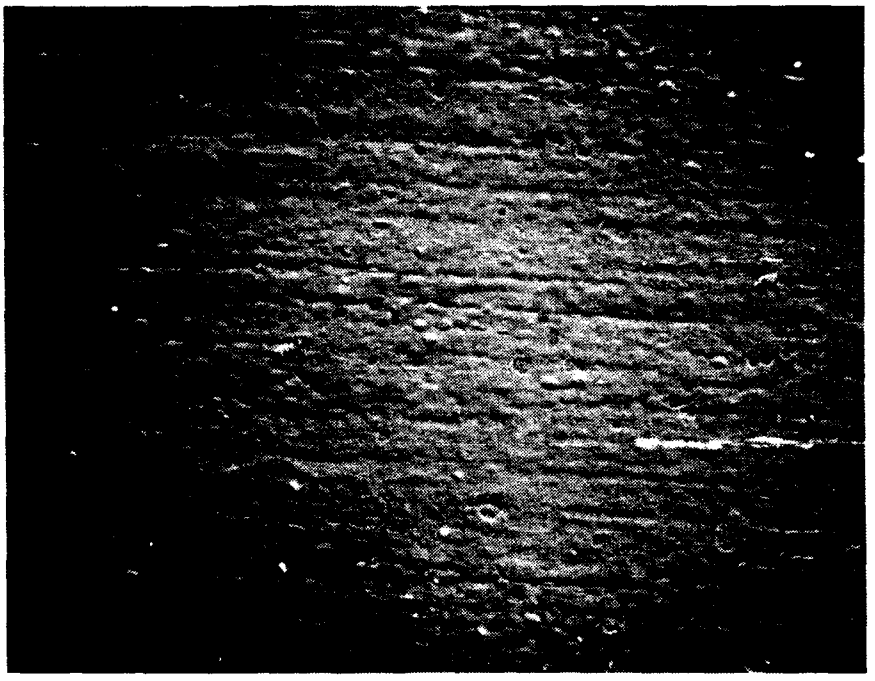

100 x

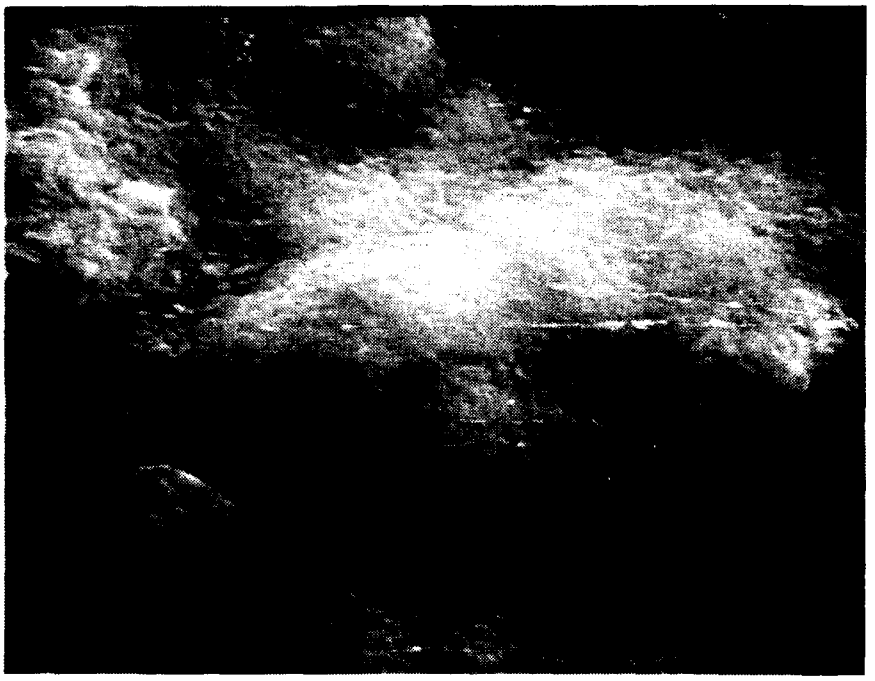

10,000 x

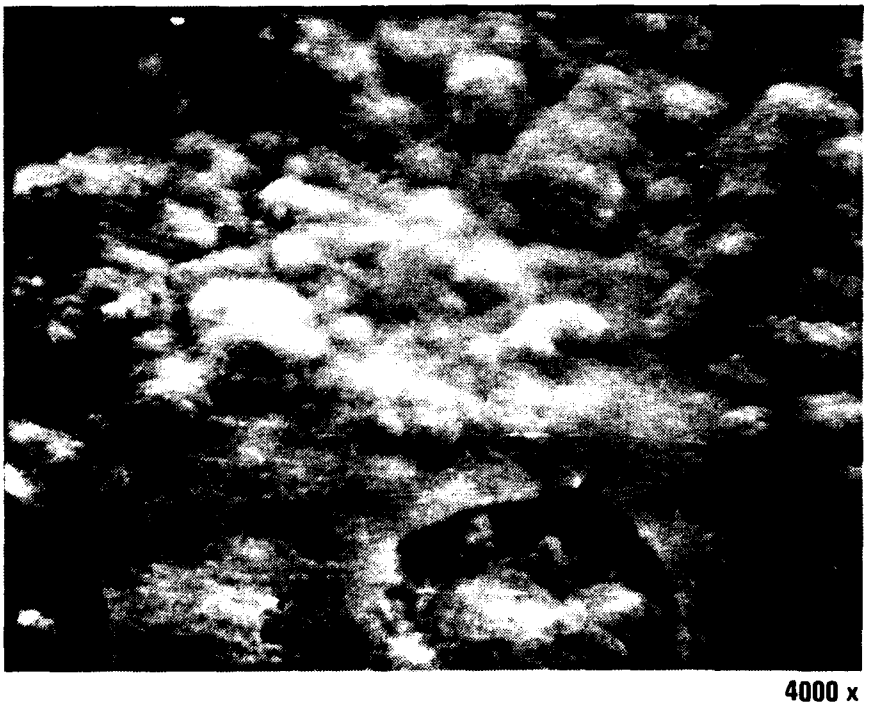

4000 x

Fig. 9. SEM photographs showing microstructure of superconducting film on yttria-coated nickel annealed at 922°C

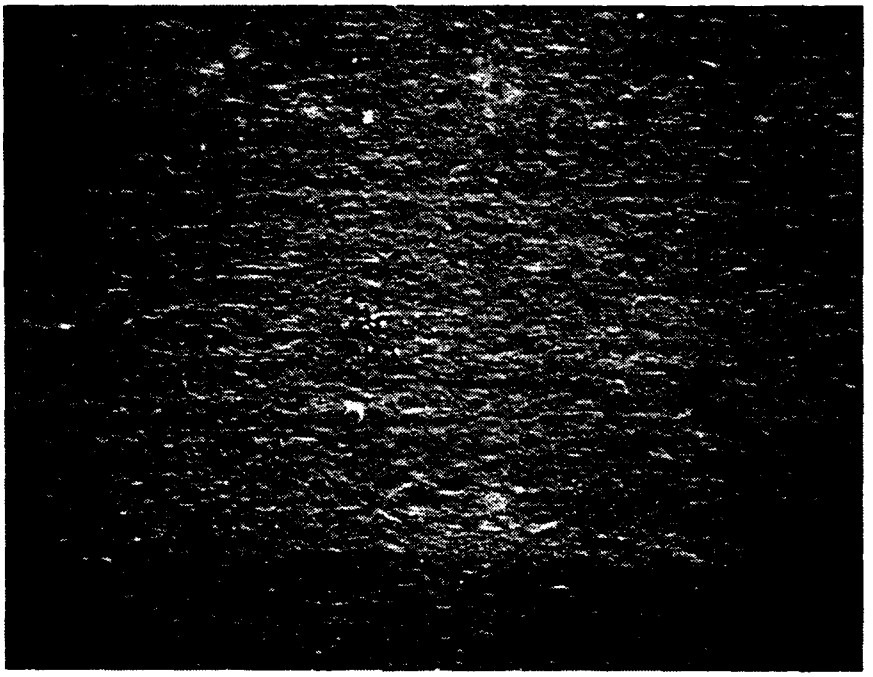

100 x

coated with film material. However, they may ultimately affect the current carrying capability of the film. The film in Fig. 6 did not exhibit a Meissner effect. This film (processed at 884°C for 60 min) has a somewhat smaller grain size, and is more dense than the superconducting film (Fig. 7) which was processed at 922°C for 10 min.

Films (Figs. 8 and 9) formed on nickel with a yttria barrier layer did not show the pock marks observed for films on YSZP. In addition, the films on the nickel substrate had a much smaller grain size than the films on YSZP. These differences may be due to a change in the precursor solution chemistry. The films on YSZP were formed from a solution which was not heated as long as the solution used to coat the nickel. Experiments are in progress to test this hypothesis.

2.2. FIBER PROCESSING

2.2.1. Resin Spinning Properties as a Function of Solvent Constituents

As stated in the previous progress report, the viscosity and spinnability of the resin was strongly influenced by the presence of different kinds of solvents as well as their relative amounts. In certain combinations, a very small change in the solvent ratio had a profound influence on the resin spinnability.

The fine-tuning of solvent content in the resin has been made and its effects on the spinning process has been examined in the resin-xylene-isopropanol system. The results were reported in the previous report. The study of the solvent constituents on the resin spinnability has been extended to resin-benzene-isopropanol system. The results are given in Table 1. This study indicates the isopropanol amount should be no more than 1.5 w/o and the amount of the benzene is close to 20 w/o. Depending on the solvent contents, the spun fibers from the cohesive resins exhibit excess, little or no die-swelling and different degrees of collapsing.

TABLE 1
CHARACTERISTICS OF RESINS IN BENZENE-ISOPROPANOL BINARY SOLVENTS

Test Run	Resin Constituents (wt%)				Resin Characteristics			
	C_6H_6	i-PrOH	Resin	Cohesive	Surface Smoothness	Die Swell	Flexibility	Collapse
B1	26.8	0.0	73.1	Yes	No	Slight	Some	No
B2	48.3	2.6	49.1	Yes	Yes	Slight	Yes	Yes
B3	39.6	2.2	58.3	No	Yes	Large	Yes	Yes
B4	25.4	1.4	73.2	Yes*	Yes	Large	Yes	Yes
B5	30.3	1.1	68.5	Yes*	Yes	No	Yes	Yes
B6	20.0	1.0	78.9	Yes*	Yes	Large	Yes	Yes
B7	18.8	1.0	81.2	Yes*	Yes	No	Yes	Slight
B8	17.8	1.0	80.2	Yes	Yes	No	Yes	No
B9	18.7	1.1	80.2	YES*	Yes	No	Yes	No

*Slightly tenacious

The effects of the solvent contents on the as spun fiber die-swelling and collapsing can be clearly seen in Fig. 10(a) through (f). In these samples, the amount of isopropanol were kept at 1 wt% and the amounts of benzene were slightly changed. The few percent variation in benzene gave rise to different degree of die-swelling and collapsing. The sample B5 had no die-swelling and a large collapsing and the sample B6 had a large die-swelling and a medium collapsing. The sample B7 and B8 had no die-swelling which is desirable. Another important property that had been examined was the draw-down ratio. This property enabled the fiber to be axially stretched to obtain smaller diameter fibers. Sample B9 demonstrated a resin with a high draw-down ratio. The fibers were stretched to obtain a smaller diameter fibers. Sample B9 demonstrated a resin with a high-down draw ratio. The fibers were stretched to 1/5 to 1/6 of the diameter of the nozzle.

While the effects of solvent constituent was clearly shown, the relation and the relative importance of the die-swelling, collapsing and drawn-down ability are still unclear. For example, from a processing point of view, a resin with large die-swelling which has a large draw-down ratio may be as good as a resin with no die-swelling and small draw-down ratio. Further studies will be performed in this area to clarify this issue.

2.2.2. Heat Treatment Schedule Study

The spun fibers had a relatively uniform diameter along the fiber length. However, the diameter of the as-spun fibers were 200 to 500 microns which were thicker than those previously reported of hand-drawn fibers with 50 to 200 microns in diameters. The larger diameter in the spun fibers poses a stringent requirement on heat treatment schedule. Therefore, the current practice is to spin a thinner fiber and, at the same time search for a new heat treatment schedule for thicker fibers. To refine the heat treatment process parameters for these fibers, it was necessary to do iterative processing of the same fiber lot at different times and temperatures schedule. It

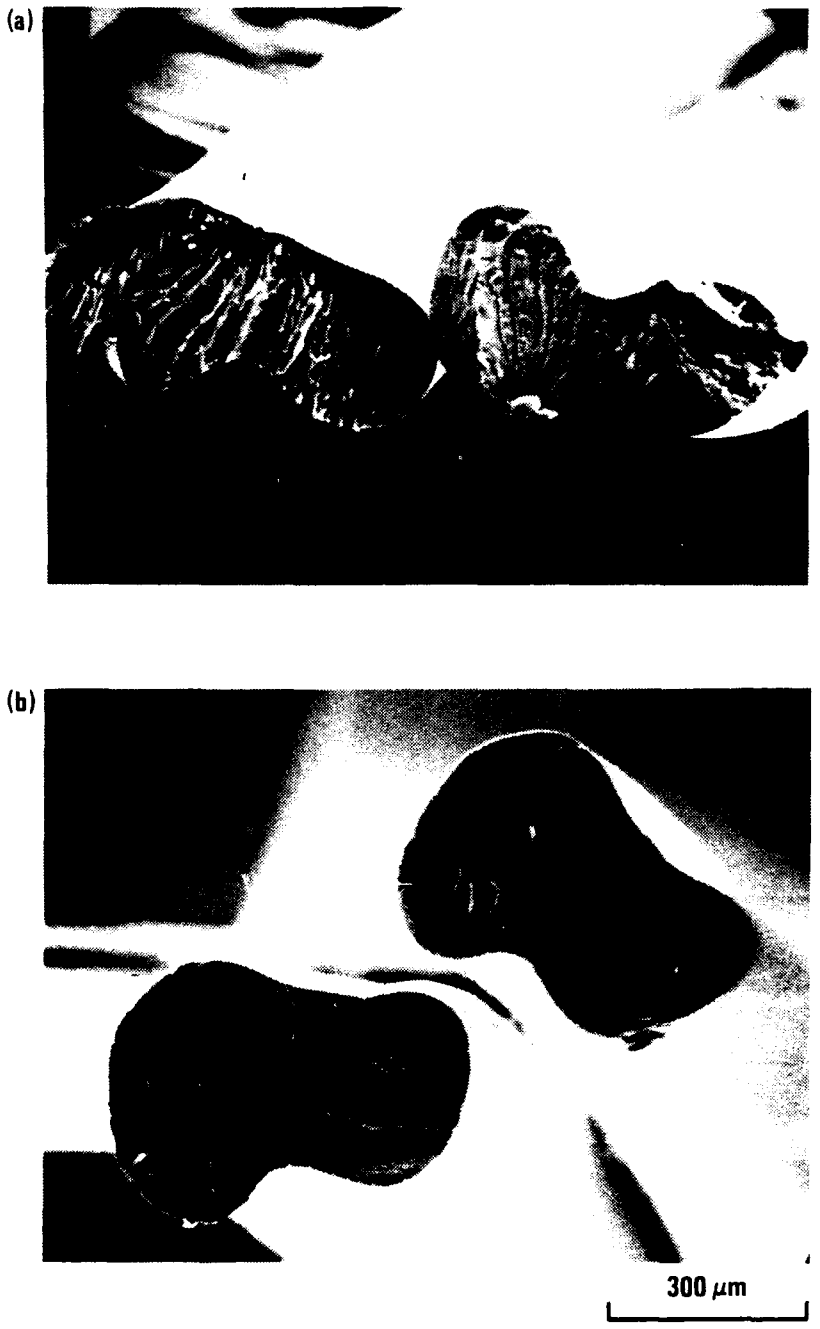

Figs. 10(a) - (f). Pre-ceramic fiber morphology showing different degree of die-swelling and collapsing; (a) sample B3: large die-swelling and large collapsing; (b) sample B5: no die-swelling, large collapsing

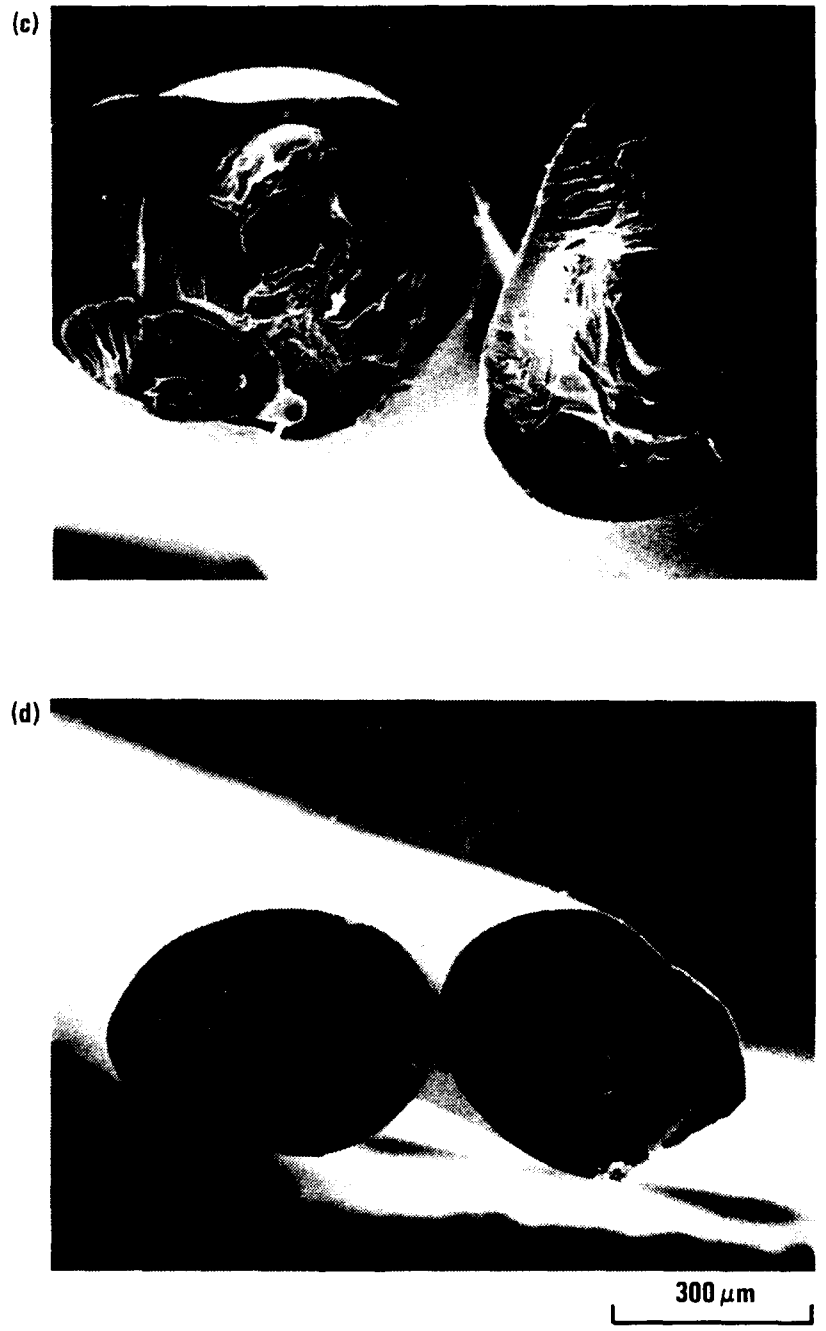

Fig. 10(c). Sample B6: large die-swelling, medium collapsing; (d) sample B7: no die-swelling, medium collapsing

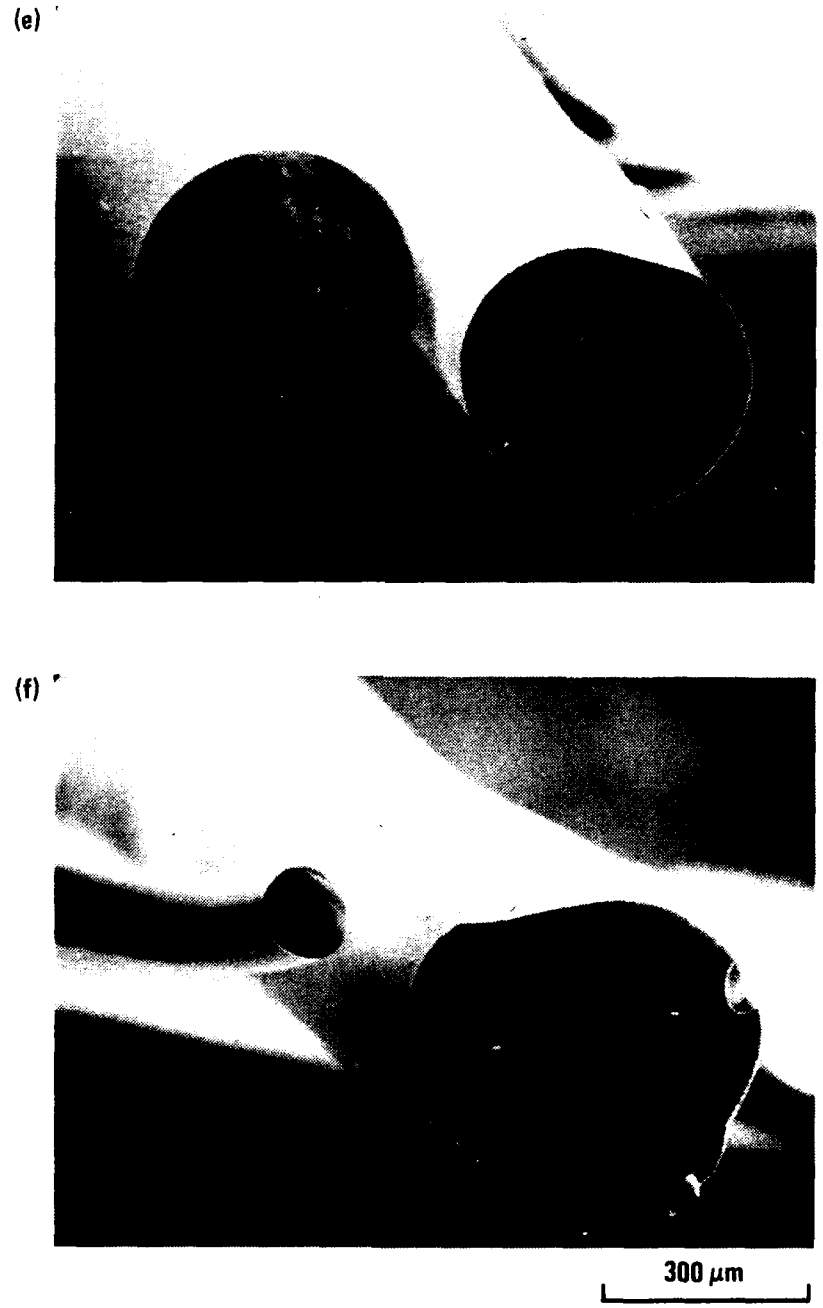

Fig. 10(e). Sample B8: no die-swelling, no collapsing; and (f) sample B9: no die-swelling, no collapsing and large draw-down ratio

was found that the first critical stage of the heat treatment was the organic removal and/or burn out between 200 and 350°C. The improper organic pyrolysis through this temperature range invariably resulted in axial crackings and weak fibers (Figs. 11 (a) through (c)). Based on the TGA of the resin shown in Fig. 12, several promising heat treatments in the range of 100° to 450°C were attempted. The polished cross sections of the fibers heat treated at one specific schedule indicated no axial cracks (Fig. 13). In order to save time for finding out proper heat treatment schedule, higher temperatures heat treatment were also performed on those fiber that did not have extensive axial cracks so that the microstructure and the superconducting properties of the fibers could be evaluated. The fibers were sintered to approximately 85 - 95% of the theoretical density. However again, the axial cracks occurred at the low temperature organic pyrolysis stage as shown in Fig. 14.

Nevertheless, the superconducting properties were evaluated by using dc magnetic susceptibility on the short fibers, and resistivity and current density measurements on longer fibers. The electrical properties of the fibers were found to be strongly dependent on the high temperature heat treatment. The superconducting onset temperature of these fibers was improved from previously reported 87 K to 92.5 K and zero resistance temperature from 81 K to 90 K. (Detailed superconducting properties of the fibers are described under the electromagnetic properties characterization.)

2.3. 123 SOLUTION COATED CERAMIC FIBERS

Another approach to obtain flexible and strong superconducting wire or fiber is to develop an adherent coating of 123 on commercially available ceramic fibers. One particular fiber (Du Pont's PRD-166) which is a zirconia alumina composite fiber has been chosen for this study. However, it has been shown that alumina, which is 80% of the selected fiber's constituent, reacts extensively with 123 material on processing at high temperatures and destroys the superconducting qualities of the coated fiber. Therefore, an effective barrier layer such as Y_2O_3 or

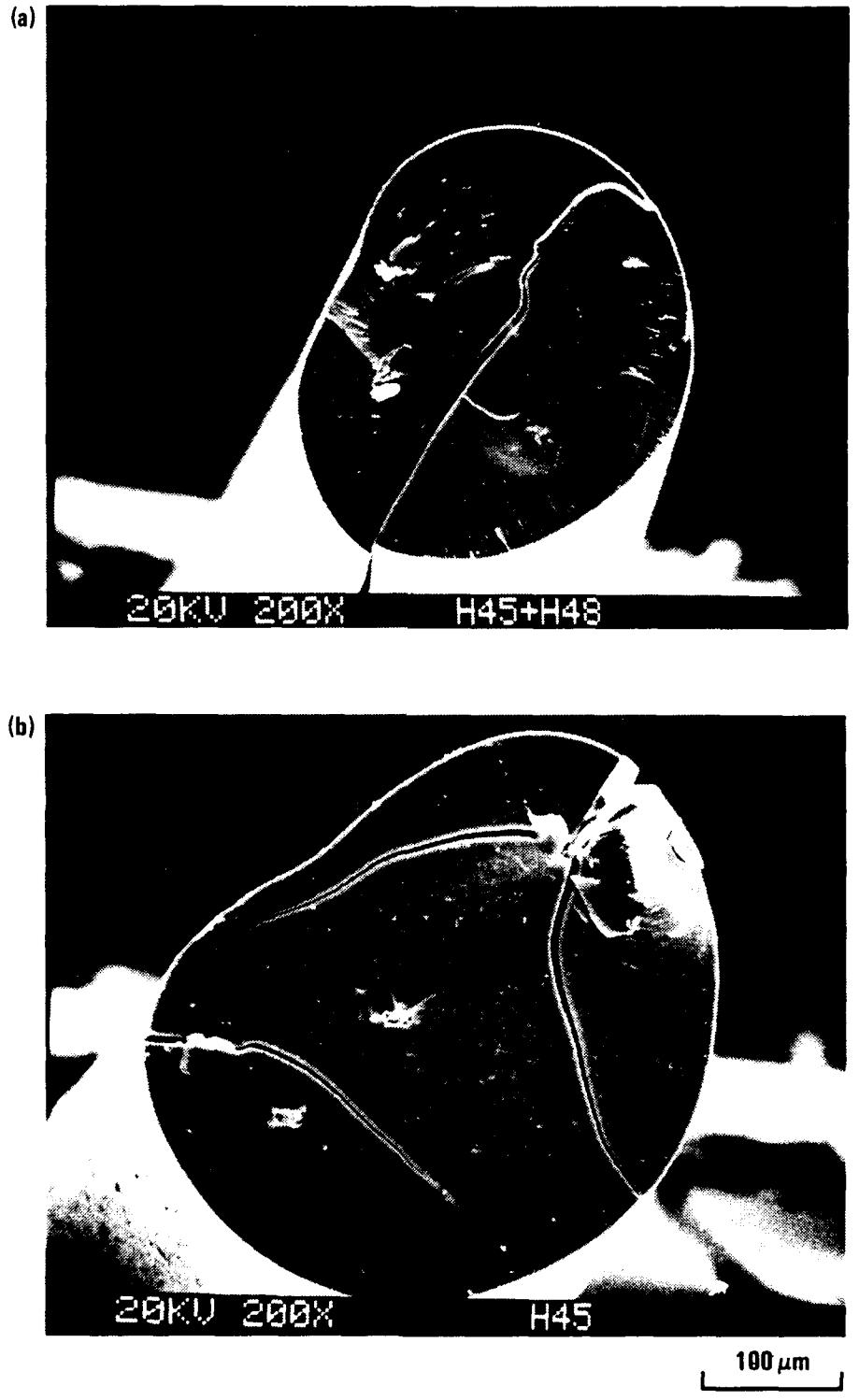

Fig. 11. Axial cracks occurred in the fibers due to the stress generated during organic pyrolysis; a) 200°C, 8 hr. b) 200°C, 8 hr and 225°C, 9 hr

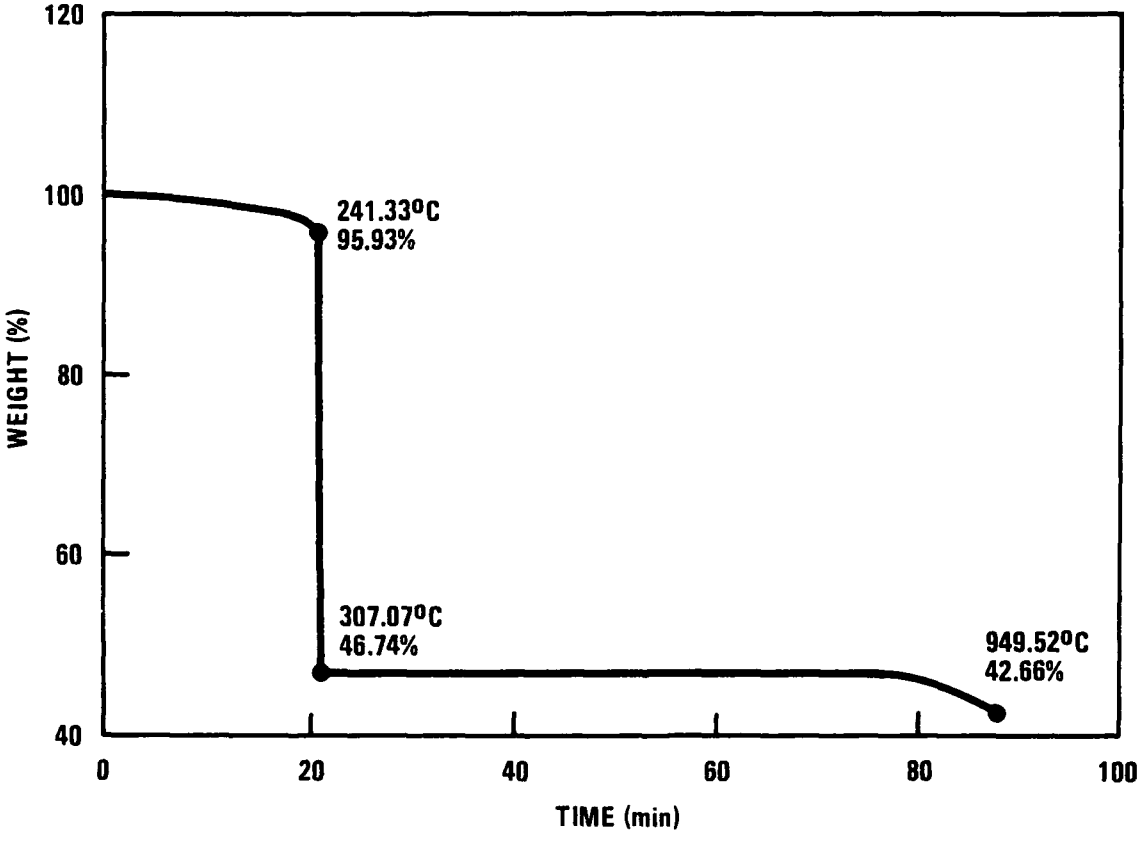

Fig. 12. TGA curve on preceramic 123 powder heated at 10 C/min

(c)

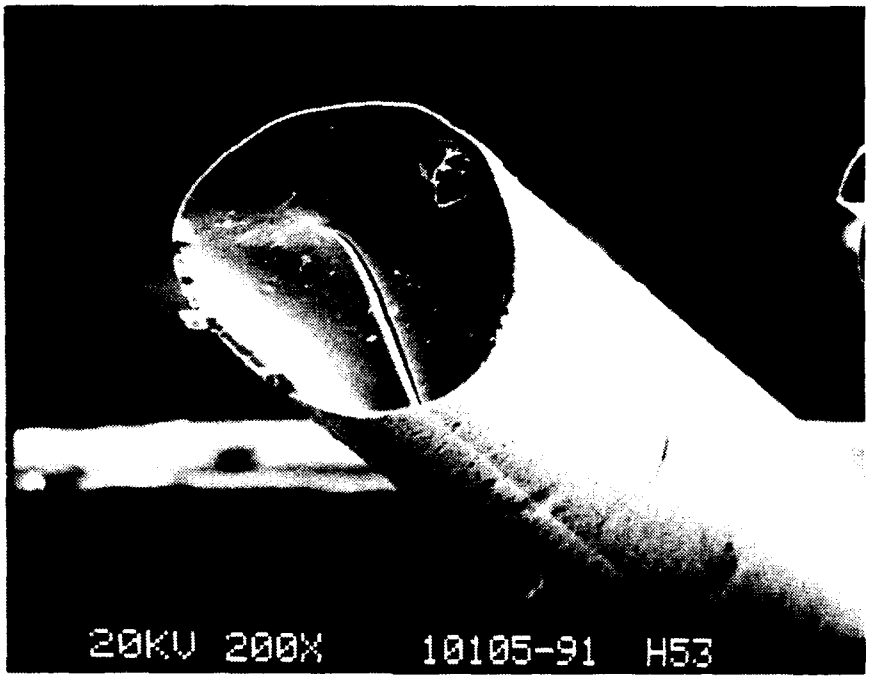

100 μm

(d)

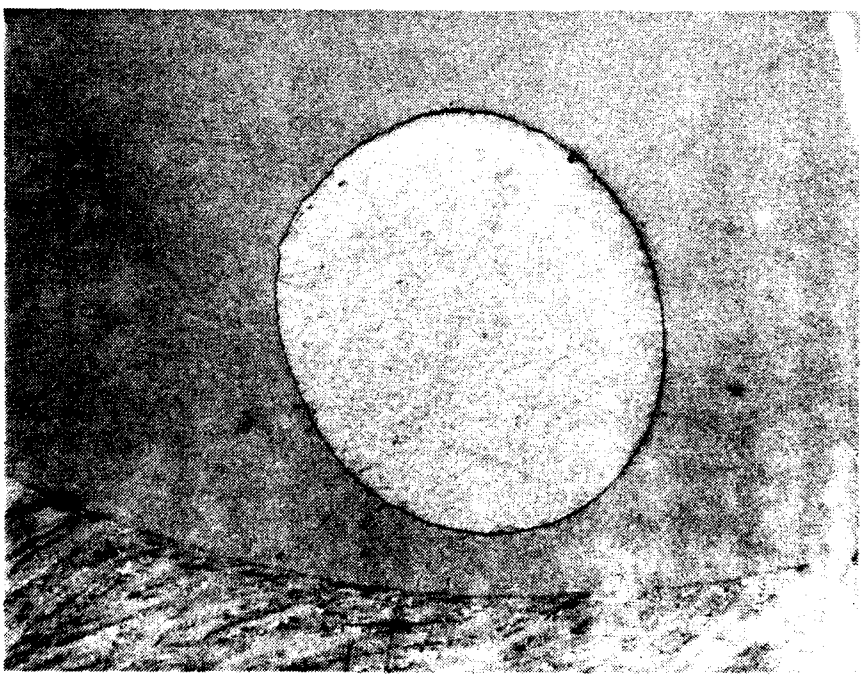

100 μm

Fig. 13. The polished cross section of fiber calcined at 180°C, 10 hr, 200°C, 8 hr and 225°C 10 hr (10105 - 85II H64)

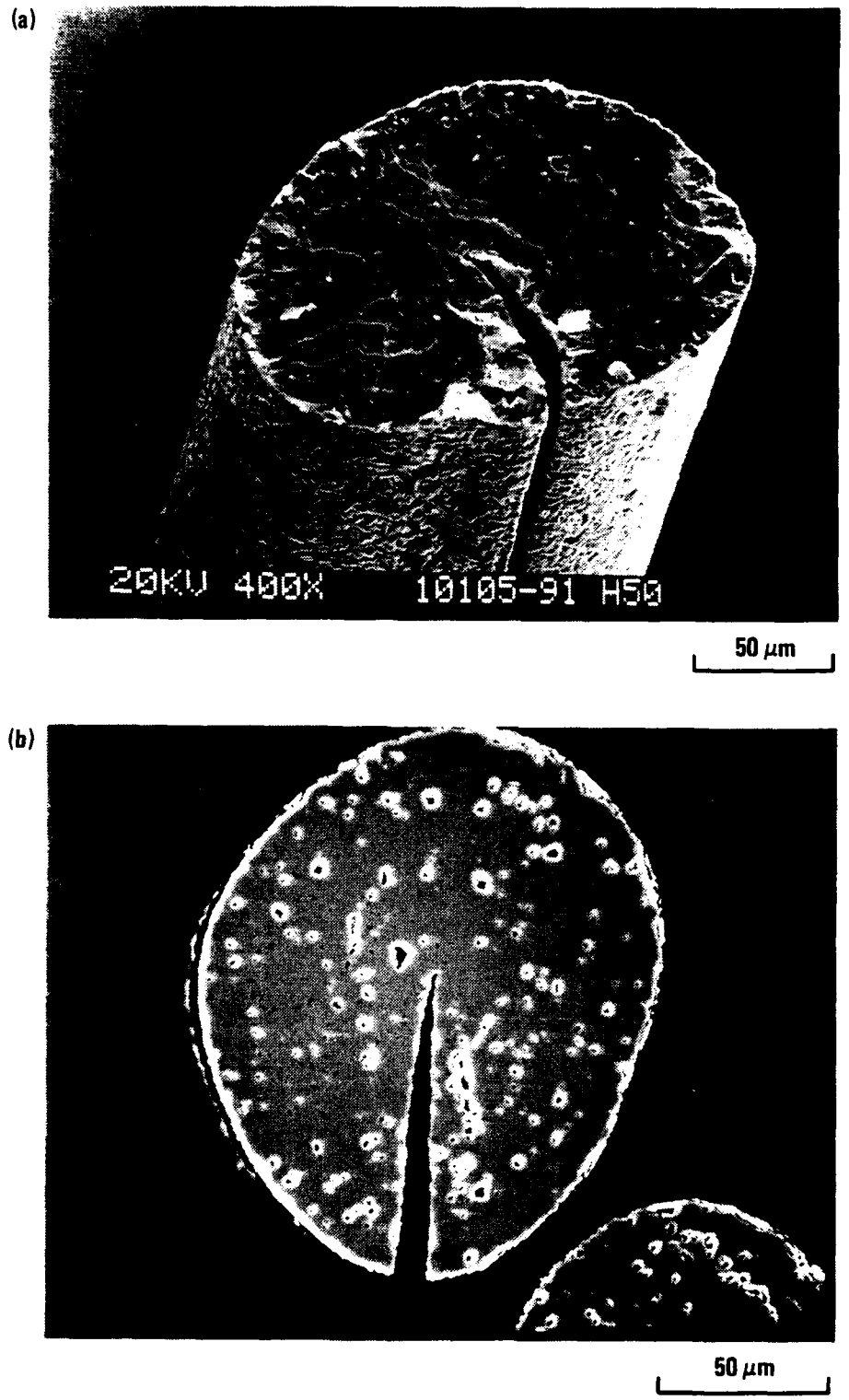

Fig. 14. Microstructrue of the fiber calcined at 905°C, 10 hr. (a) Fractured cross section and (b) polished cross-section.

$LaAlO_3$ is needed to inhibit the interaction between the fiber and the 123 material. But the small 5-10 μm diameter fibers are found difficult to handle and hand coat and characterize. Thus, pure alumina substrate was used instead for a demonstration feasibility study. In order to verify the effectiveness of the aforementioned barrier coatings, pure alumina substrates were coated with Y_2O_3 and $LaAlO_3$ by sol-gel method and X-ray diffraction analysis were performed to determine the presence and phase purity of the coated substrates.

2.3.1. Sol-Gel Derived $LaAlO_3$

The aluminum and lanthanum isopropoxides were prepared as described in the literature (Ref. 3). The lanthanium concentration was determined by EDTA titration and the aluminum content was the calculated average based on the amount of alumina content from three aluminum alkoxide samples.

Two batches of La/Al isopropoxides were prepared and mixed in exact proportion to give oxide molar ratio of $LaAlO_3$. The mixed alkoxides were refluxed for 1 hr under an N_2 purge. One batch was hydrolyzed with an excess amount of H_2O to white mixed lanthanum and aluminum hydroxides. The aluminum-lanthanum hydroxides formed were dried under vacuum to white powder. A Small amount of the powder was heat treated at various temperatures starting from 900°C to a temperature at which single $LaAlO_3$ phase was formed. The XRD pattern of the powder prepared is shown (Fig. 15). Another batch was divided into small portions and stored in septum vials for fiber coating.

2.3.2. Y_2O_3 Sol-Gel Coated Alumina and PRD-166 Fibers

Alumina substrates were manually coated with 2 different concentrations (0.017M and 0.055M) of Y(OPr)3 inside the glove box. The less concentrated (0.017M) was also repeatedly coated onto the same substrates using the automatic dip coater. it was found that highly concentrated solutions do not lend themselves well to automatic dip

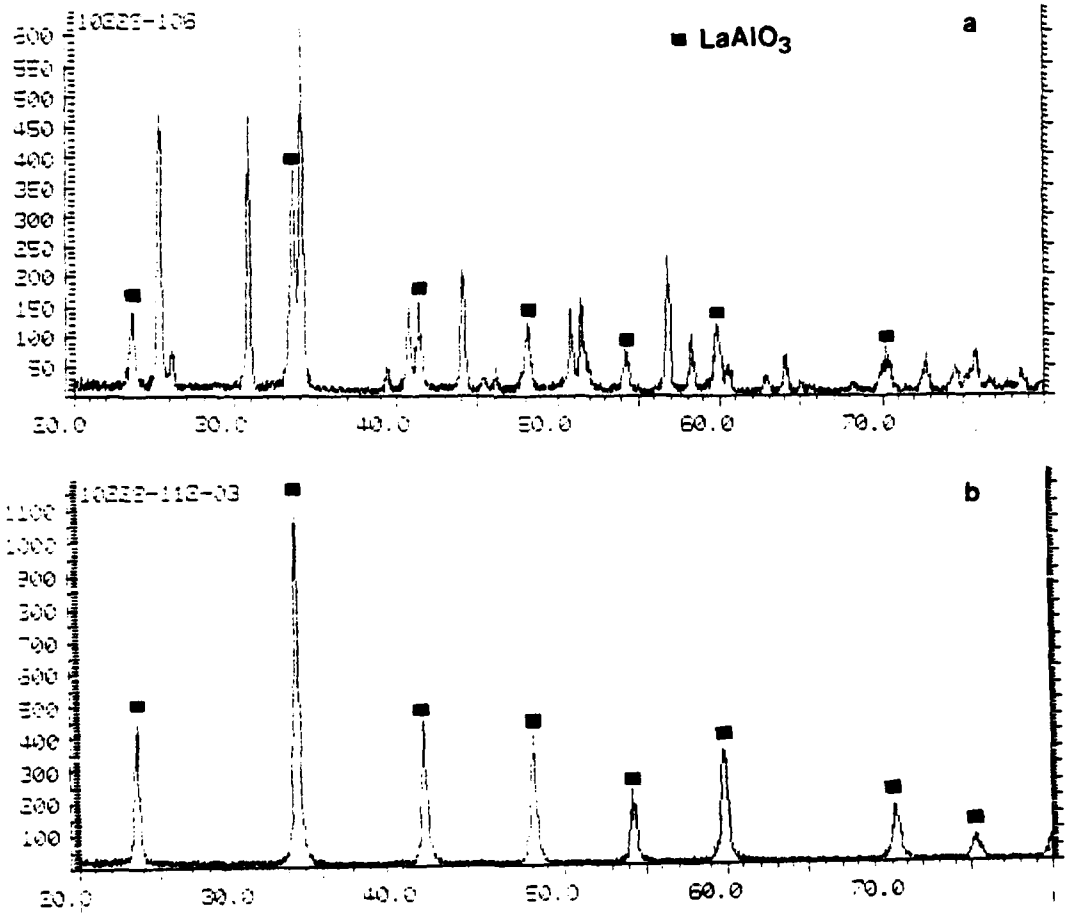

J–548(5)
4–26–90

Fig. 15. X-ray diffraction patterns for the composition La203: A1203 = 1:1 after heat treatments at (a) 900°C, and (b) 100_0 ZC for 1/2 hr

coater because they hydrolyze readily in the less controlled environment of the dip coater. Thus, the alkoxides were hydrolyzed while drying the substrate in ambient atmosphere between each dipping. Coated samples were then fired in air to 900°C for 1/2 hrs.

The amounts of alumina and yittria phases were determined using EDAX. Table 2 summarizes the results obtained for the coated substrates. Based on the preliminary results, it was decided to coat all subsequent alumina substrates and fibers 10 times using the dip coater. The X-ray diffraction pattern of the coated substrates showed the presence of Y_2O_3 as shown in Fig. 16.

2.3.3. $LaAlO_3$ Sol-Gel Coated Alumina Substrates and PRD-166 Fibers

$LaAlO_3$ sol were repeatedly, and up to 10 times were coated onto the alumina substrates as before. X-ray analysis of the coated samples after heat treatment at various temperatures (900, 1000, and 1100°C) for 1/2 hr exhibit similar patterns as shown in Fig. 15. Since very small amounts of $LaAlO_3$ were detected by EDAX after firing the sample at 900°C, it was evident that additional dipping cycles are necessary to produce a barrier layer of satisfactory thickness. Thus subsequent samples were coated 15 times rather than ten times.

2.3.4. 123 Solution Coated Al_2O_3 Coated Substrate

Using the dip coater, approximately 20 wt% of 123 precursor was dissolved in mixture of toluene and isopropanol and used, for coating the alumina coated substrates. The resistivity measurements of the fired samples are in progress.

TABLE 2
EDAX RESULTS OF Y_2O_3 COATED ALUMINA SUBSTRATES

Method	Hand Dipped		Dip Coater	
Concentration	0.017M	0.055M	0.017M	0.017M
Time	10	6	9	5
Y203	6 - wt%	9 - 10 wt%	10 - 13 wt%	7 wt%

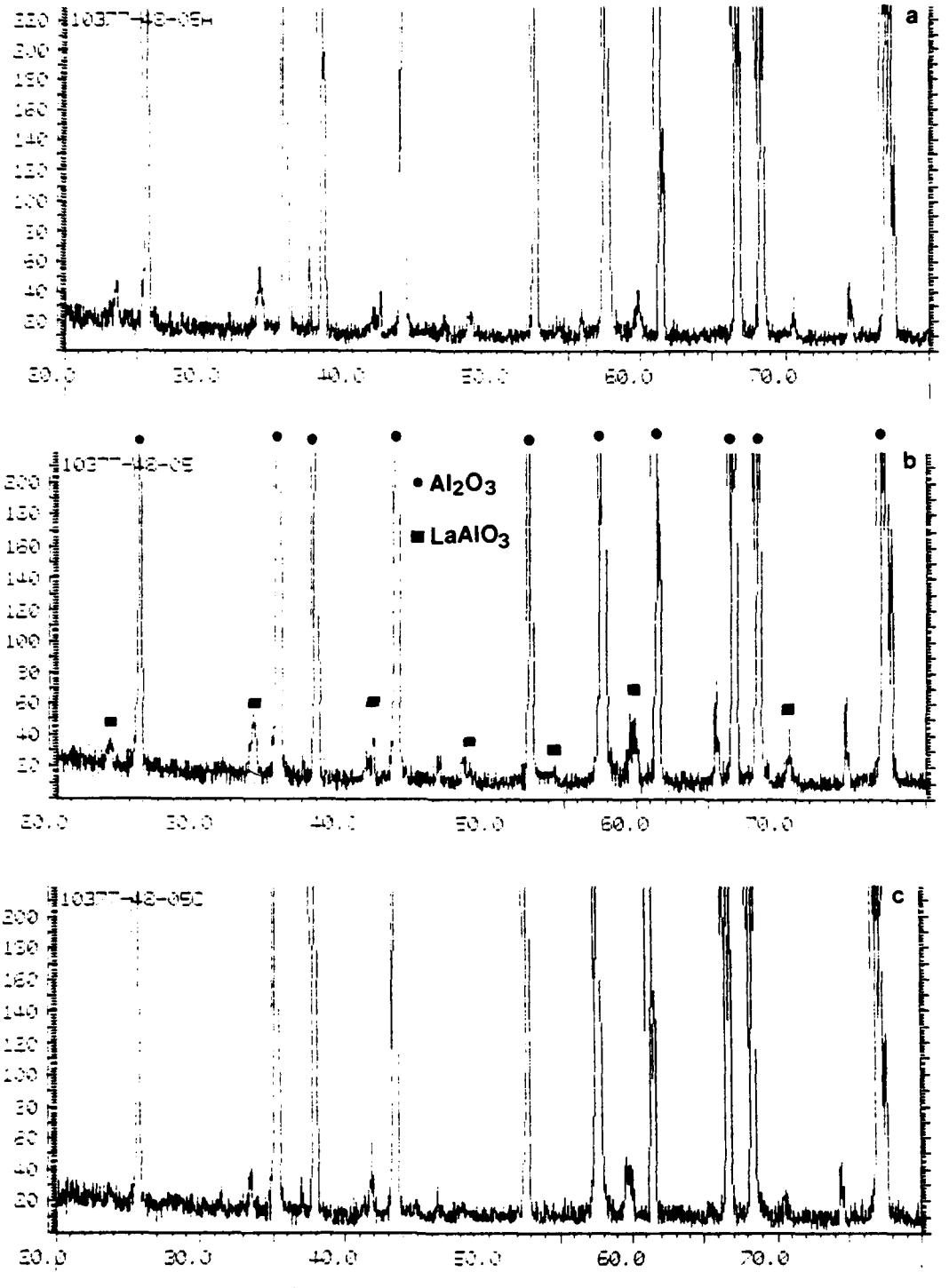

J–548(4)
4–26–90

Fig. 16. X-ray diffraction patterns of LaA103 coated alumina substrates after heat treatments at various temperatures (a) 900°C, (b) 1000°C, and (c) 1100°C.

3. ELECTROMAGNETIC PROPERTIES

3.1. FIBER

Magnetic property measurements on a number of $YBa_2Cu_3O_7$-δ fibers were performed with a Quantum Design MPMS SQUID susceptometer. Typical data is shown in Fig. 17, in which the magnetic susceptibility is plotted as a function of temperature. After the sample was cooled in zero field to 5 K, a field of 1 gauss was applied, and the sample was heated to 120 K. Finally, the sample temperature was returned to 5 K. The onset of superconductivity occurred at ~90 K and the transition had a width of $\Delta T \simeq T_{90} - T_{10} = 10$ K. The ratio of the field cooled susceptibility to the zero field cooled susceptibility was ~0.31, indicating that a minimum of 31% of the sample was superconducting.

Figure 18 shows the resistivity as a function of temperature for $YBa_2Cu_3O_7$-δ fiber. The fiber is superconducting with a critical temperature of $T_c \quad T_{50} = 91.5$ K, and a transition width, $\Delta T \quad T_{90} - T_{10} = 1.5$ K. Thus, both magnetic and transport measurements yield excellent superconducting transitions.

The critical current density of the fibers was measured at 77 K in the absence of a magnetic field. The sample diameter was 0.0114 cm, and the distance between the voltage leads was 0.29 cm. In Fig. 19, the voltage is plotted as a function of current. The critical current, determined when one μV/cm voltage drop occurred across the voltage leads, was found to have a density of ~70 amps/cm^2. The relatively low critical current density at this temperature indicates that conduction between the grains need to be substantially improved. In addition, the presence of any impurity phases in the fibers could be expected to have a significant impact on the transport properties because of the relatively small fiber cross section.

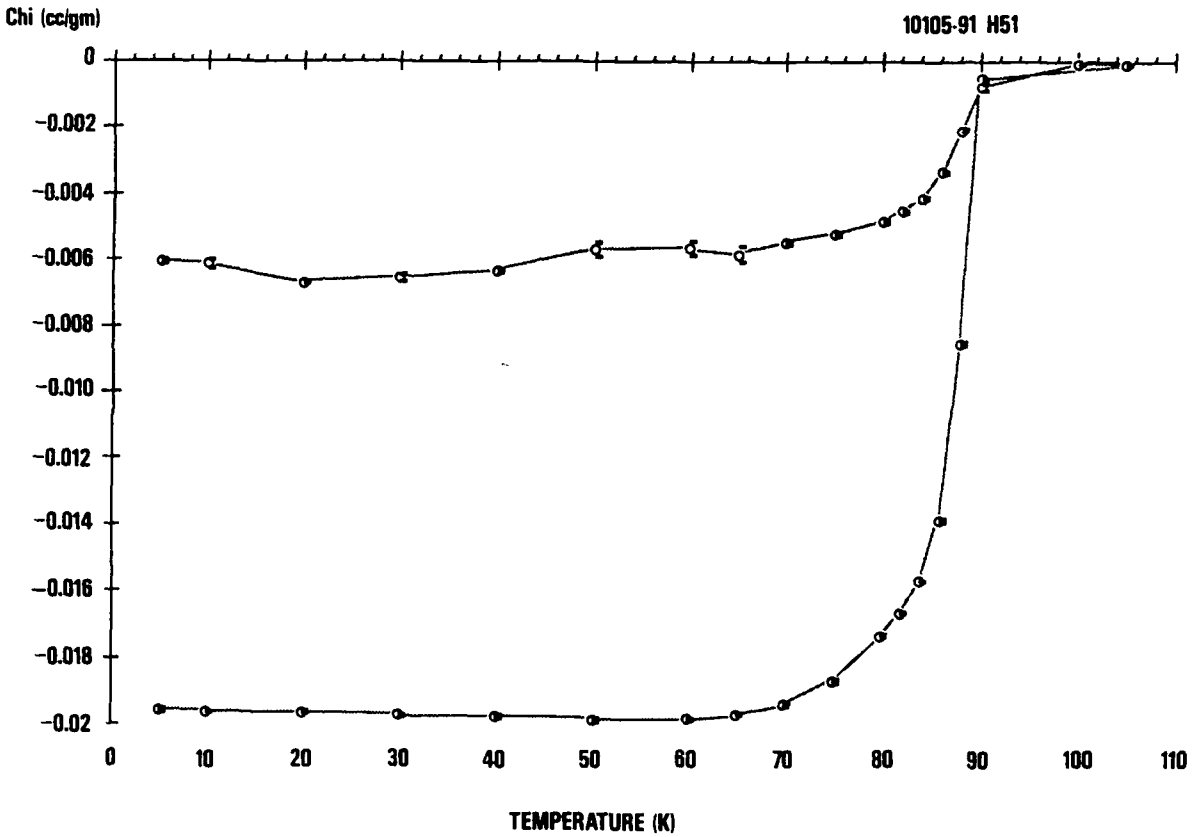

J–484(3)
4–4–90

Fig. 17. DC magnetic susceptibility as a function of temperature for an $YBa_2Cu_3O_{7-\delta}$ fiber. After the sample was cooled in zero field to 5 K, a field of 1 gauss was applied. The temperature was increased to 120 K and decreased to 5 K. The superconducting transition occurred with an onset at ~90 K and a width of $\Delta T \quad T_{90} - T_{10} = 10$ K.

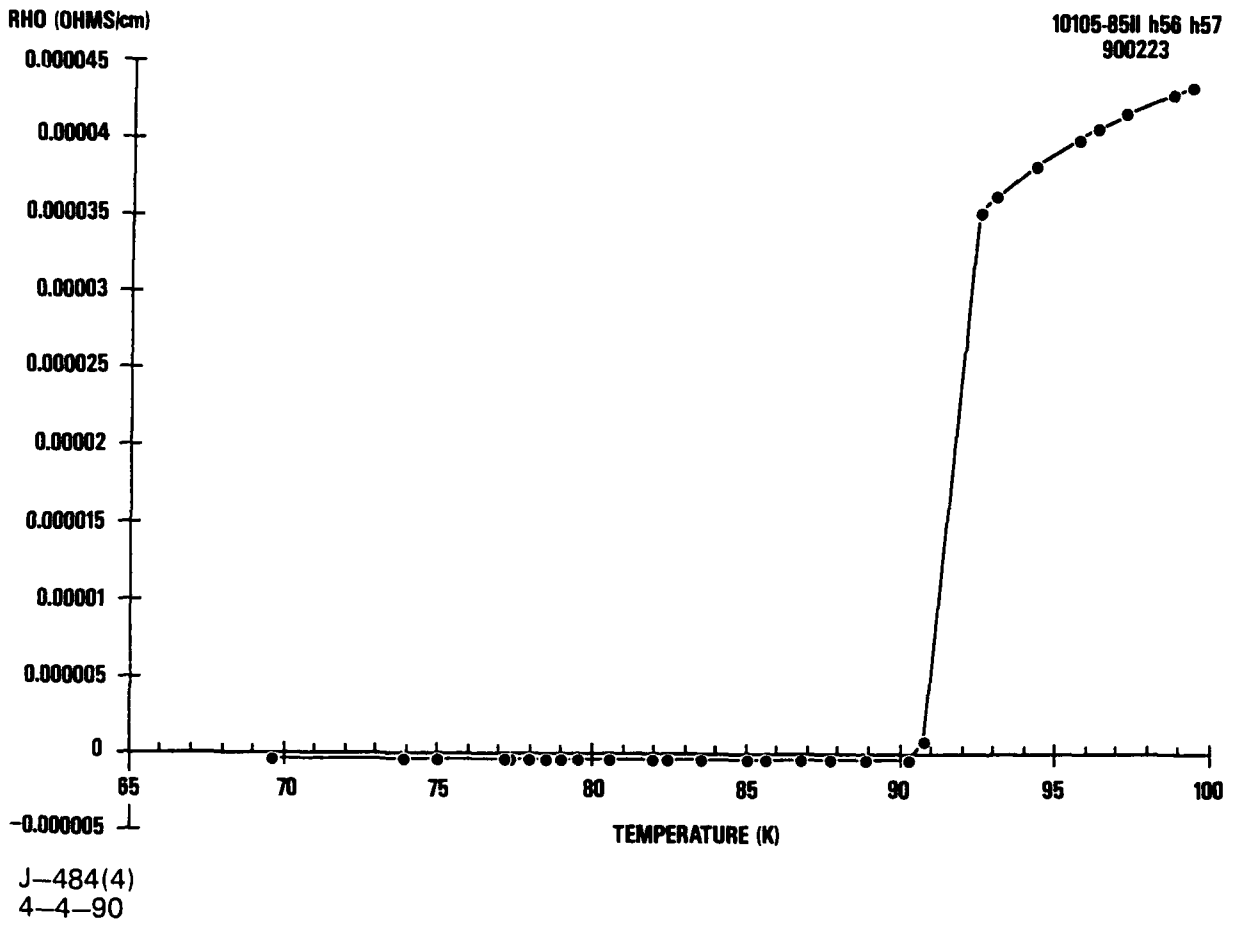

Fig. 18. Resistivity as a function of decreasing temperature for an $YBaCu3O_{7-\delta}$ fiber. The superconducting transition occurred with a midpoint at 91.5 K and a width of 1.5 K.

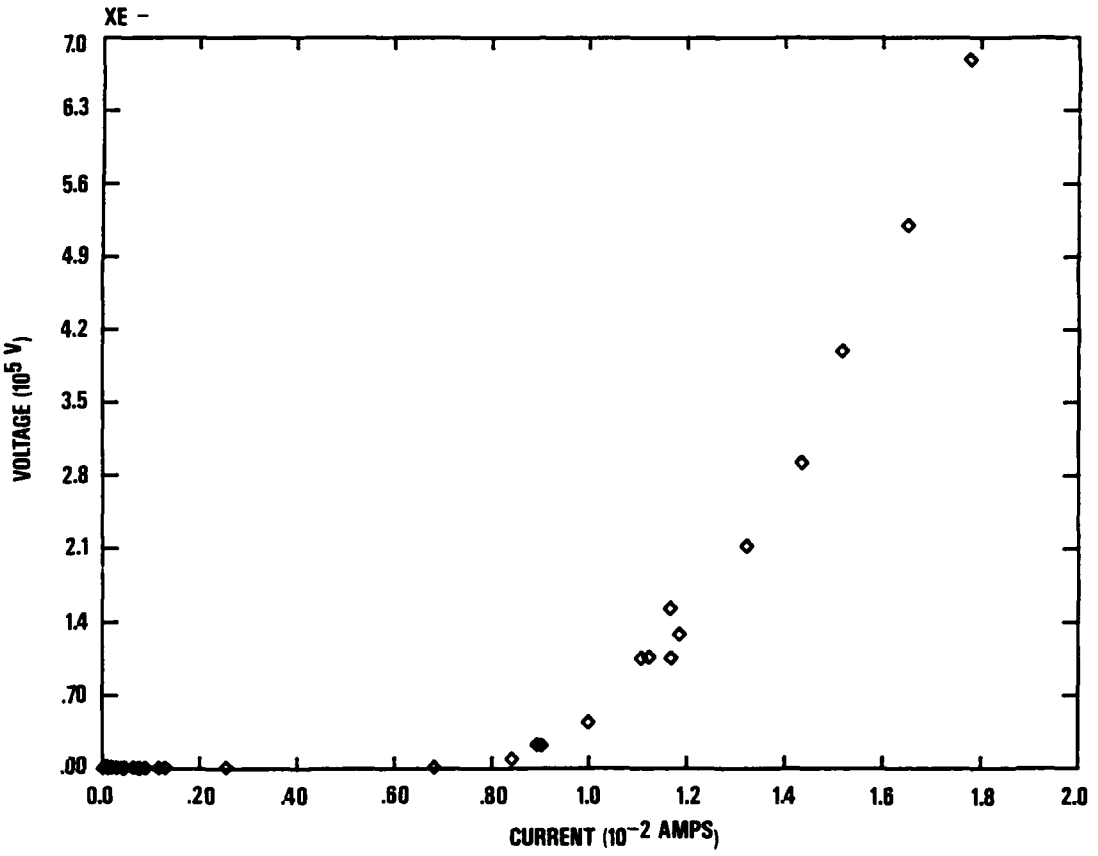

J–484(2)
4–4–90

Fig. 19. Voltage as a function of current for an $YBaCu3O_{7-\delta}$ fiber at 77 K in the absence of an applied field. The critical current density when 1 μV/cm occurred across the voltage leads was ~70 A/cm^2

3.2. EXTRUDED ROD

Figure 20 shows typical data for the magnetic susceptibility as a function of temperature in a magnetic field of 1 guass for a $YBa_2Cu_3O_7$-δ extruded rod. The sample exhibits an onset of superconductivity above 90 K and a transition width less than 2 K. The ratio of the field cooled to zero field cooled susceptibility is 0.58, indicating that a minimum of 58% of the material is superconducting.

As shown in Fig. 21, the resistance of a $YBa_2Cu_3O_7$-δ extruded rod was measured as a function of temperature. The sample was found to be superconducting with a critical temperature of 90 K and a transition width of $<$ 5 K.

The critical current density was measured for an extruded rod with a diameter of 0.71 cm. The distance between voltage leads was 0.449 cm. Figure 22 shows the voltage as a function of current. A value of 250 Amps/cm^2 was found.

Thus, the extruded rods exhibit excellent superconducting properties as determined by magnetic and transport measurements. We believe that the improved critical current may be related to the larger cross-sectional area and the dense microstructure of the rods.

3.3. THIN FILMS

The dc magnetic susceptibility of $YBa_2Cu_3O_7$-δ thin films prepared by sol-gel dip coating method on yttria-stabilized zirconia polycrystal was measured in a field of 30 guass. Figure 23 shows the susceptibility as a function of temperature, where the contribution of the substrate, extrapolated from the measured susceptibility in the normal sate, has been subtracted. The sample showed an onset of superconductivity between 80 K and 90 K, and a transition width of about 5 K.

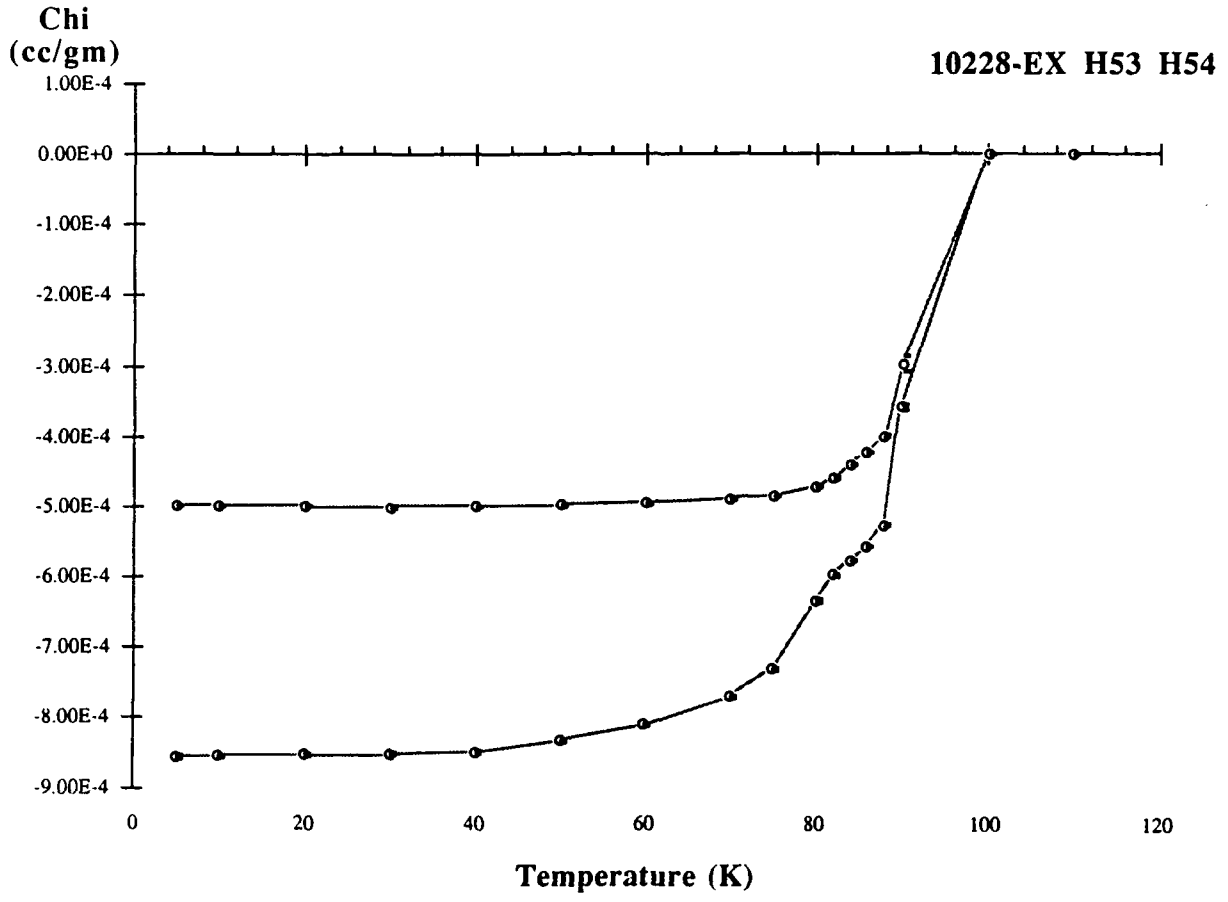

Fig. 20. Magnetic susceptibility as a function of temperature for an $YBaCu3O_{7-\delta}$ extruded rod. The sample was cooled in zero field to 5 K, a field of 1 gauss was applied, and the sample was heated to 110 K and cooled to 5 K. The superconducting transition occurred with an onset above 90 K and a width <22 K.

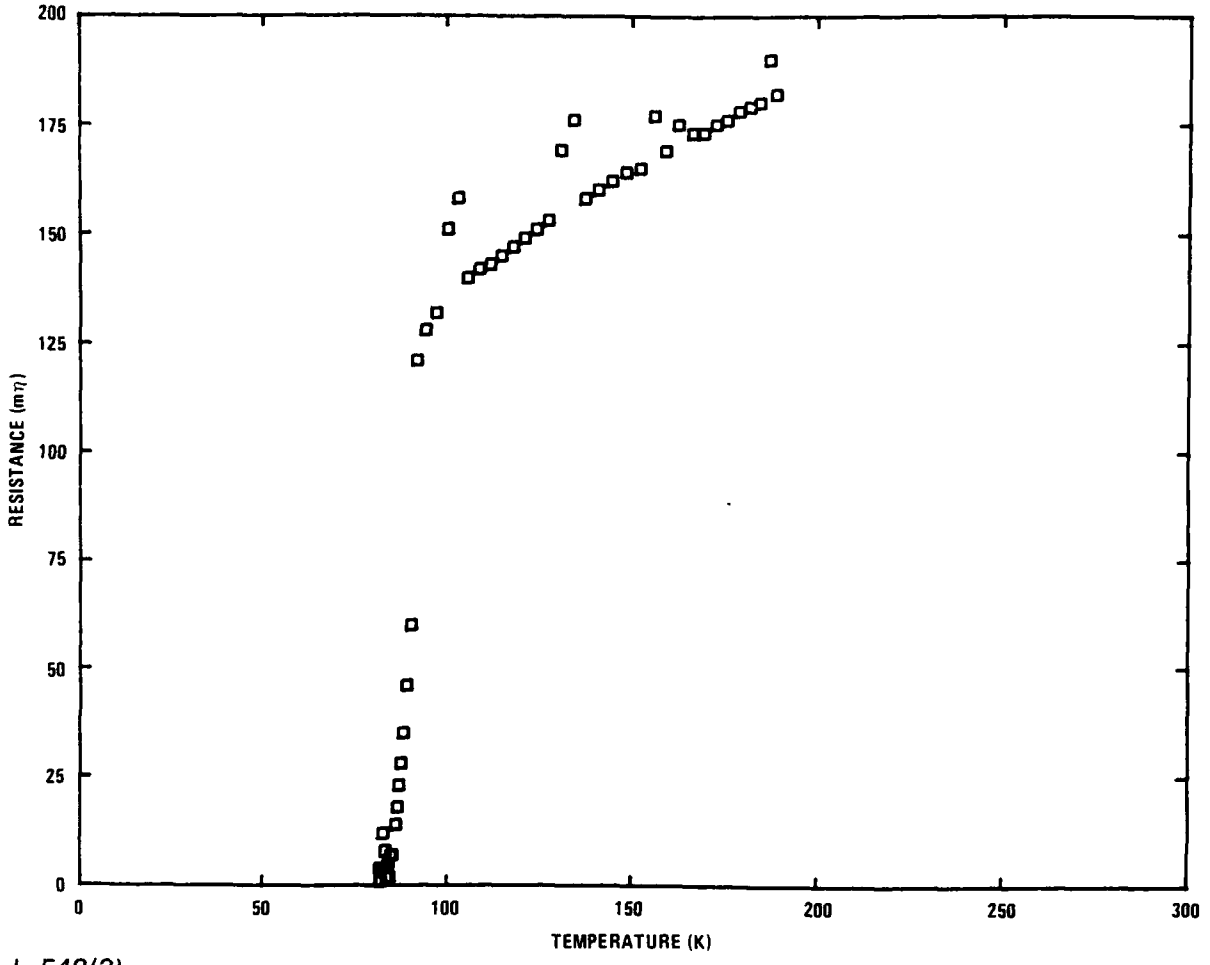

J–548(2)
4–26–90

Fig. 21. Resistance as a function of temperature for an $YBaCu3O_{7-\delta}$ extruded rod. The superconducting transition occurred with a midpoint at 90 K and a width of <5 K.

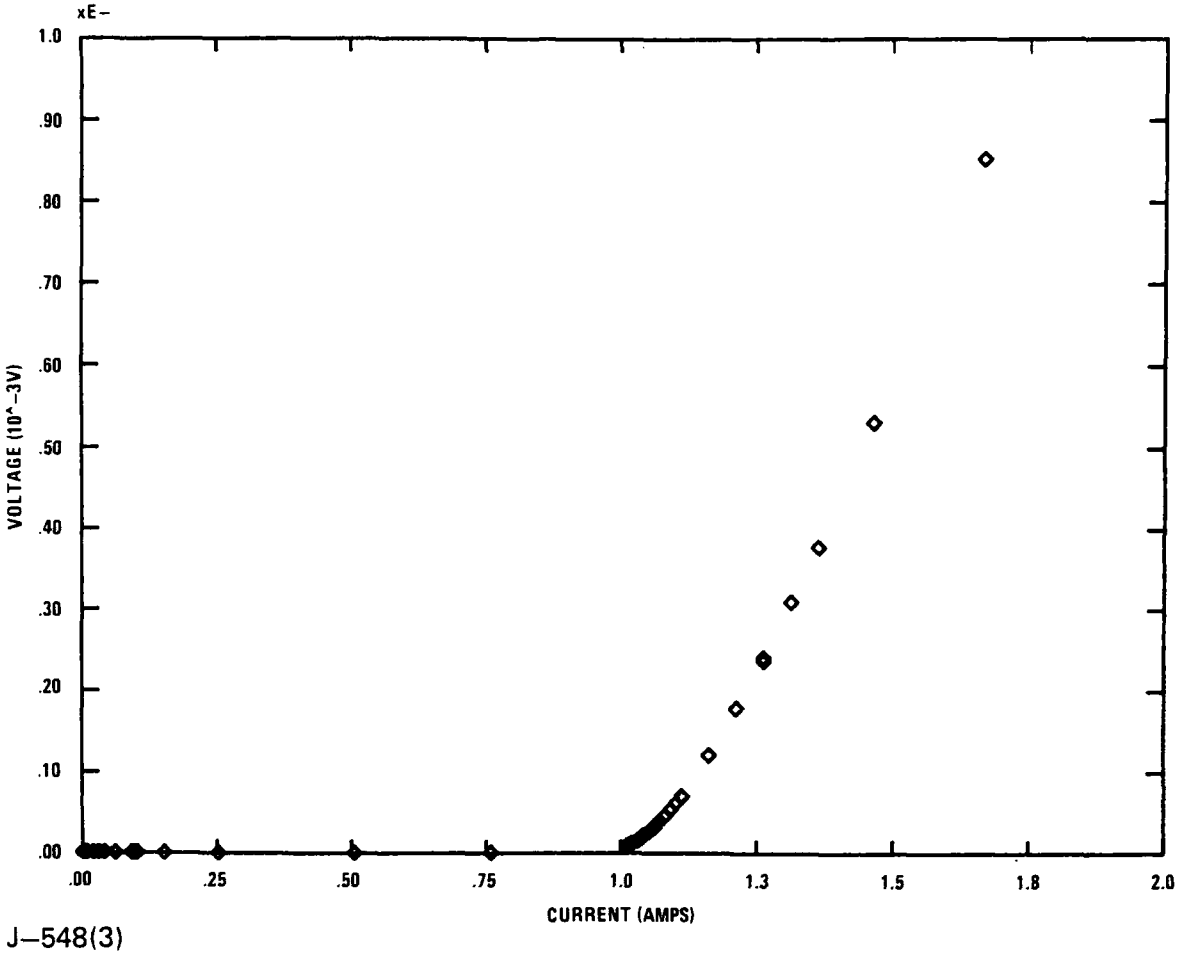

Fig. 22. Voltage as a function of current for an $YBaCu3O_{7-\delta}$ extruded rod at 77 K in the absence of an applied field. The critical current density when 1 μV/cm occurred across the voltage leads was 250 A/cm^2.

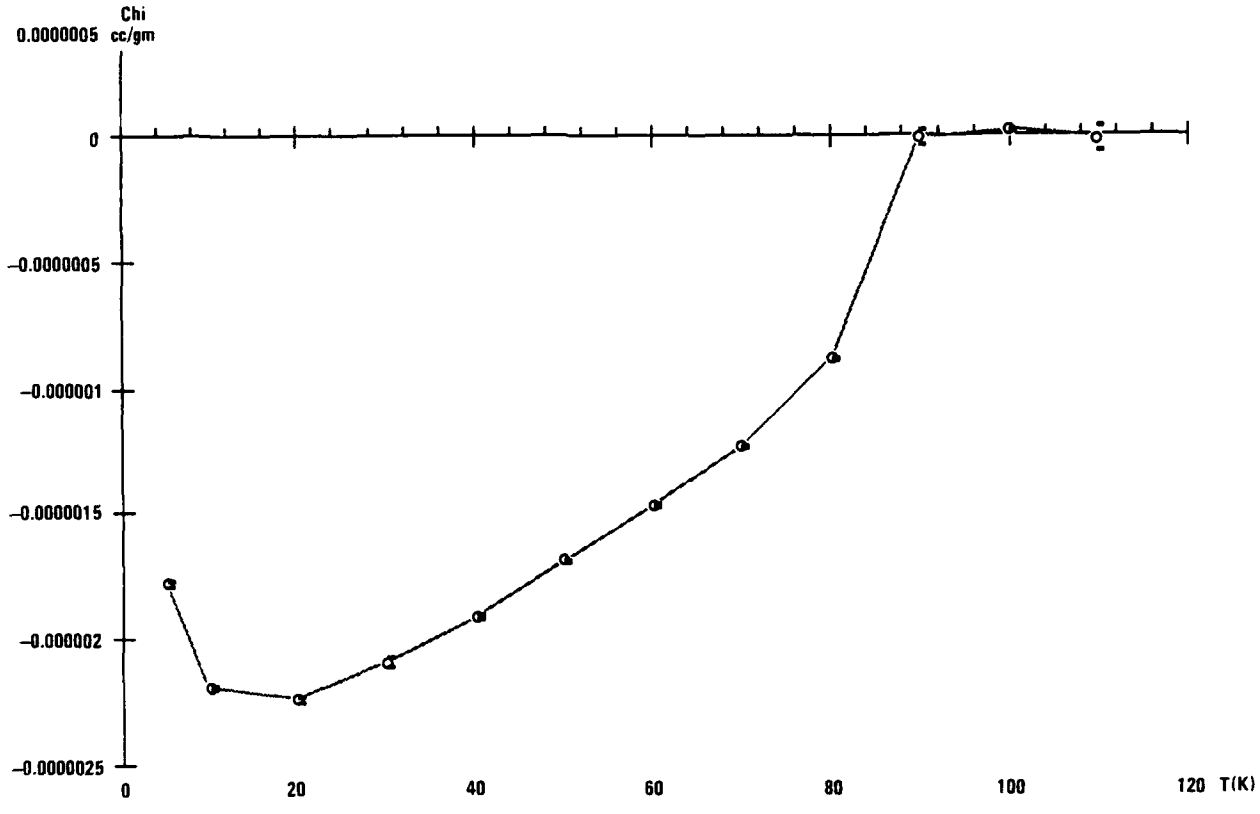

J-548(1)
4-26-90

Fig. 23. Magnetic susceptibility as a function of temperature for an $YBaCu3O_{7}$-δ thin film. The contribution from the YSZ substrate was subtracted. The sample was cooled in an applied field of 1 gauss. The superconducting transition occurred with an onset >80 K and a width ~5 K.

Resistance measurements have also been performed on a number of these films. Many samples show a decrease in resistance below 60 to 70 K, and zero resistance has been achieved as hign as 38 K. All of the samples show a normal state resistivity that increases with decreasing temperature.

At the present, we are about to determine the composition of several thin films using electron microprobe analysis. Since the films interact with the substrate, the composition may be very strongly affected by the high temperature processing and annealing procedure, and we are optimistic that these studies will yield information that will enable us to improve the quality of the films. Annealing procedures that have been used up to this point have involved relatively long times (10 min to 1 hr) above 900°C for optimal grain growth. At these temperatures, significant interactions with the substrate can be expected to occur, and we plan to experiment with shorter annealing times.

4. CAVITY Q FACTOR MEASUREMENT

An all copper cavity, consisting of two end plates and an open cylinder just like a metal cavity coated on the inside with high temperature superconducting ceramic (HTSC), was constructed and the temperature dependence of the Q was obtained. The Q was 24,000 at 77 K and 39,000 at 4.2 K and the resonant frequency was 10.9 GHz.

A fixture for measuring the surface resistance of small (0.5" or 0.75" diameter) HTSC coated silver disks is being fabricated. The first disks will be coated and their surface resistance measured in April.

A kit for screening up to four superconducting films by obtaining the temperature dependence of the ac magnetic susceptibility is being purchased from Lakeshore Cryogenics, Inc. The kit will be integrated with the cryogenic dewar already purchased for this program and an IBM PC-compatible computer as soon as it arrives.

5. REFERENCES

1. Fahrenholtz, W. G., D. M. Millar and D. A. Payne, "Preparation of $YBa_2Cu_3O(7-x)$ from Homogeneous Metal Alkoxide Solution," Advanced Ceramic Materials, preprint.

2. Nishi, Yoshitake, et. al., "High T_c of $TBa_2Cu_3O_x$ Coated Film on a Nickel Plate Annealed for a Short Period," J. of Materials Science Letters, 8, 1989, 1362-1364.

3. Mazdiyasni, K. S., "Powder Synthesis from Metal-Organic Precursors," Ceramic International, 8(2), 42-56 (1982).